

An Introduction to Webs

C.D. WHITE^{a1}

^a School of Physics and Astronomy, Scottish Universities Physics Alliance, University of Glasgow, Glasgow G12 8QQ, Scotland, UK

Abstract

Webs are sets of Feynman diagrams that contribute to the exponents of scattering amplitudes, in the kinematic limit in which emitted radiation is soft. As such, they have a number of phenomenological and formal applications, and offer tantalising glimpses into the all-order structure of perturbative quantum field theory. This article is based on a series of lectures given to graduate students, and aims to provide a pedagogical introduction to webs. Topics covered include exponentiation in (non-)abelian gauge theories, the web mixing matrix formalism for non-abelian gauge theories, and recent progress on the calculation of web diagrams. Problems are included throughout the text, to aid understanding.

1 Introduction

One of the purposes of quantum field theory is the calculation of scattering amplitudes, which are related to the probability for a given particle collision to occur. Typically, amplitudes are calculated in perturbation theory, and it is well known that such calculations are beset by infinities. Some of these infinities (ultraviolet divergences) can be absorbed into redefinitions of the Lagrangian parameters defining the theory, a procedure known as *renormalisation*. In these lectures, we will be concerned with infrared (IR) divergences, which correspond to long distance physics.

That long distance physics is associated with divergences in perturbation theory can be inferred by examining figure 1. This depicts a $2 \rightarrow 2$ scattering process, in which one of the outgoing particles emits a gluon. This emission may be *real*, in which case the gluon itself ends up as a final state particle. Alternatively it may be *virtual*, in which case it joins up again with the outgoing particle. These two possibilities are shown in figure 1(a) and (b) respectively. The Feynman rules for emission of a gluon tell us to integrate over all possible positions for the end of the gluon. That is, there is an integral

$$\int d^d x \dots$$

in d space-time dimensions. Because one integrates out to infinite distance, there will always be some value of d above which this integral diverges, and in fact this is found to be $d = 4$. Hence,

¹Christopher.White@glasgow.ac.uk

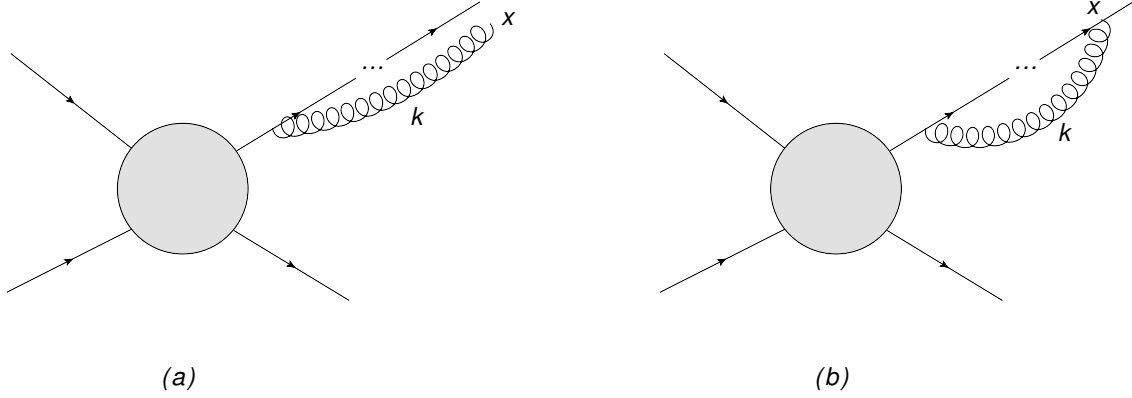


Figure 1: Emission of a gluon of momentum k from an outgoing particle in a scattering amplitude: (a) real emission; (b) virtual emission.

singularities associated with long distance physics are a crucial ingredient in practical applications of field theory.

Note that a gluon that extends out to infinite distance has an infinite Compton wavelength. Thus, by the uncertainty principle, such a gluon has a vanishing momentum or energy $k^\mu \rightarrow 0$. This is the origin of the phrase “infrared divergences” for long distance singularities - if we were calculating Feynman diagrams such as those in figure 1 in momentum space, the singularities would show up after integrating over the emitted gluon momentum k^μ , as contributions from the region where this tends to zero in all components. Such gluons are referred to as *soft* in the literature, as opposed to *hard* particles which have nonzero momenta.

From figure 1, we also see that if a gluon has an infinite Compton wavelength, it is difficult to distinguish between the case of real or virtual emission, as a virtual gluon will only rejoin an outgoing particle at infinity. Thus, both real and virtual diagrams will contain infrared singularities (after integrating over the gluon position in the real case), and we expect that the real and virtual contributions for a given soft gluon will be closely related to each other. This is indeed the case, and in fact IR divergences cancel upon combining real and virtual graphs. Furthermore, this is guaranteed, for suitably defined quantities, to all orders in perturbation theory [1]. However, large residual contributions to observable quantities remain, which typically take the form of terms such as

$$\alpha_S^n \frac{\log^m E}{E} \quad (1)$$

involving logarithms of the total energy E carried by soft gluons. Such terms occur at all orders $\mathcal{O}(\alpha_S^n)$, and are highly divergent as $E \rightarrow 0$ such that perturbation theory breaks down in this regime. Close to this limit, the logarithmic terms are not formally singular, but can be numerically large. Then perturbation theory is no longer sufficiently convergent for a truncation at e.g. next-to-leading order to be sensible. One must then sum up the terms of eq. (1) to all orders in the coupling constant, a procedure known as *resummation*. This is by now a highly developed field - see e.g. [2–12] for several different approaches, and refs. [13, 14] for recent review articles. Implicit

in the above discussion is that resummation is intimately linked with the structure of infrared singularities to all orders in perturbation theory.

Infrared singularities are also of interest in themselves. In particular, there are a number of recent conjectures regarding IR divergences in a variety of theories. One example is the so-called *dipole formula* in QCD [15–19], an all-order ansatz for the IR singularities of fixed-angle scattering amplitudes with massless particles. There is also interesting recent work on singularity structures in supersymmetric gauge theories, and their relationship to similar amplitudes in (super-)gravity [20–25]. The IR singularity structure of quantum gravity itself has been studied in [26], and more recently in [27–30]. The relation between QCD and gravity in the soft limit has been explored in [31], and used to provide evidence for the *double copy* conjecture relating both theories [20,21].

As a result of these investigations, much is already known about the structure of infrared divergences. Crucially, it is known that scattering amplitudes *factorise* into the following schematic form [32–38]:

$$\mathcal{A} \sim \mathcal{H} \cdot \mathcal{S} \cdot \prod_{i=1}^L \frac{J_i}{\mathcal{J}_i}. \quad (2)$$

Here the left-hand side represents an amplitude with a fixed number L of outgoing hard particles, where it is assumed that ultraviolet renormalisation has already taken place. The first factor on the right-hand side is the *hard function*, and is finite in four dimensions (i.e. contains no IR singularities). We can think of this as a subamplitude for the outgoing hard particles, where no soft gluons are emitted. The second factor \mathcal{S} is the *soft function*, and collects all singularities associated with gluon emissions whose 4-momenta each tend to zero. The final factors, one for each outgoing particle, collect *collinear singularities*, i.e. divergences associated with gluons emitted parallel to a given outgoing hard particle, in the case that this is massless. We will not be concerned with these here, but let us briefly remark that J_i is called a *jet function*, and contains collinear singularities associated with outgoing particle i . Because gluons can be soft and collinear at the same time, one double counts these singularities by including them both in the soft function \mathcal{S} and the jet functions $\{J_i\}$. One corrects for this double counting by dividing by *eikonal jet functions* \mathcal{J}_i , which can be thought of as the jet functions J_i evaluated in the soft limit.

From now on we focus exclusively on the soft function \mathcal{S} which, as described above, collects all singularities arising from multiple gluon soft gluon emission, including overlapping soft / collinear divergences. We will see that the soft function has a Feynman diagram interpretation *by itself*, so that it will be possible to calculate the soft function independently of the particular details of a given hard scattering process (other than the number of hard outgoing particles, and their momenta). Furthermore, we will see that the soft function \mathcal{S} has an exponential form, such that one may schematically write

$$\mathcal{S} \sim \exp \left[\sum_n \alpha^n c_n \right], \quad (3)$$

where α is the coupling constant, and the $\{c_n\}$ are coefficients which depend upon the momenta of the hard outgoing particles. This formula is a highly useful result, for the following reason: because soft gluon corrections appear in an exponent, they are summed up to all orders in perturbation theory. Expanding the exponential as a Taylor series in α gives terms to infinite order, where

IR divergent contributions at higher orders are related to singularities at lower orders. Successive terms in α in the exponent sum up successive towers of divergent contributions in the perturbation series. We see, then, that exponentiation is crucial to the resummation of soft gluon contributions, and that the problem of classifying IR divergences to all orders in perturbation theory is equivalent to the study of the exponent of eq. (3).

We can go further than this. It turns out that, in both abelian and non-abelian gauge theories (as well as perturbative quantum gravity), the *exponent* of \mathcal{S} can be given a Feynman diagram interpretation directly. That is, the coefficients c_n can be obtained from a special class of Feynman diagrams. The particular properties these diagrams have depend on which theory we are considering. For now, we will refer to any such diagram as a *web*:

A *web* is a diagram that contributes to the exponent of the soft function.

We will make this definition more precise (and even revise it) in the various theories to be examined in what follows, but this first definition of a web efficiently encapsulates the main idea. Before examining specific theories, it is useful to motivate why webs are useful in the first place. There are a number of reasons, which include the following:

1. By definition, webs allow one to compute the exponents of soft gluon amplitudes directly. This is in contrast to the traditional way of calculating the exponent at a given order, which is to subtract from the (unexponentiated) amplitude those terms which arise from the exponentiation of lower order terms. This involves a large amount of unnecessary work, and it is much more efficient to be able to work directly in the exponent.
2. Webs are, in an important sense, complete Feynman diagrams. Thus, some finite contributions may exponentiate as well as parts which are formally singular. Such finite contributions can be numerically large in many scattering processes, so that resummation of them is a useful means of increasing the precision of theoretical predictions.
3. Recent work has begun to generalise factorisation formulae beyond the pure soft gluon approximation (also referred to as the *eikonal approximation* for the outgoing hard particles) [12, 39–54]. Webs may be an essential ingredient of this programme in the most general case.
4. Webs, and their associated mathematical structures, may give new insights into the structure of IR singularities in a variety of theories, including in particular QCD and $\mathcal{N} = 4$ Super-Yang-Mills theory.
5. There are links between webs in non-abelian gauge theories and interesting problems in the field of enumerative combinatorics. Some of these problems may have practical applications in computer science, thus there is potentially an intriguing possibility that lessons from quarks and gluons can be applied to e.g. network transfer protocols, or search algorithms.
6. Recent progress hints at systematic methods for computing web diagrams [55–64]. This offers the hope of being able to compute all-order properties in the *exponents* of amplitudes, which constitutes an unprecedented look at intricate structures in perturbation theory.

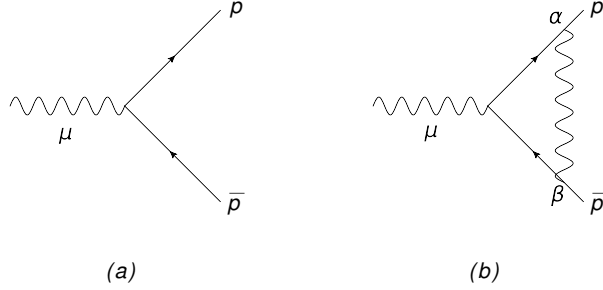


Figure 2: Amplitude for an offshell photon decaying to a fermion-antifermion pair: (a) leading order; (b) dressed with a single photon emission.

Having introduced the basic idea of webs, and also having hopefully conveyed why they might be useful, let us now begin to examine the simplest case of webs - namely, the exponentiation of soft photon corrections in abelian gauge theory.

2 Abelian Exponentiation

In this section we consider QED, and show in a specific example that soft photon contributions exponentiate, where the exponent can be interpreted directly in terms of a type of Feynman diagram. This analysis is similar to that originally carried out in [65].

We begin by considering the simple scattering amplitude shown in 2(a), consisting of an (off-shell) photon decaying into a massless fermion / anti-fermion pair. We label the 4-momenta of the latter by p and \bar{p} respectively, as shown in the figure. Ignoring coupling factors for brevity, the amplitude in momentum space is given by

$$\mathcal{A}_0 = \bar{u}(p)\gamma^\mu v(\bar{p}), \quad (4)$$

where μ is the Lorentz index of the offshell photon. Let us now consider adding a single photon emission, as shown in figure 2(b). The corresponding amplitude is

$$\mathcal{A}_1 = \bar{u}(p)\gamma^\alpha \frac{(\not{p} - \not{k})}{(p-k)^2} \gamma^\mu \frac{(\not{k} - \not{\bar{p}})}{(k-\bar{p})^2} \gamma^\beta v(\bar{p}) D_{\alpha\beta}(k), \quad (5)$$

where $D_{\alpha\beta}(k)$ denotes the photon propagator, and we do not show explicitly the integral over the gluon momentum k . One may now consider the soft limit $k \rightarrow 0$. In this limit, we can ignore the factors of \not{k} in the numerator of eq. (5), and neglect the k^2 terms in the denominators. Using also the fact that $p^2 = 0$, one finds

$$\mathcal{A}_1 \rightarrow \bar{u}(p)\gamma^\alpha \frac{\not{p}}{-2p \cdot k} \gamma^\mu \frac{\not{\bar{p}}}{2\bar{p} \cdot k} \gamma^\beta v(\bar{p}) D_{\alpha\beta}(k), \quad (6)$$

We can simplify this expression by using the anticommutation property of the Dirac matrices, $\{\gamma^\mu, \gamma^\nu\} = 2g^{\mu\nu}$, to write

$$\bar{u}(p)\gamma^\alpha \not{p} = -\bar{u}(p) \not{p}\gamma^\alpha + 2p^\alpha \bar{u}(p) \quad (7)$$

$$\not{\bar{p}}\gamma^\beta v(\bar{p}) = -\gamma^\beta \not{\bar{p}}v(\bar{p}) + 2\bar{p}^\beta v(\bar{p}). \quad (8)$$

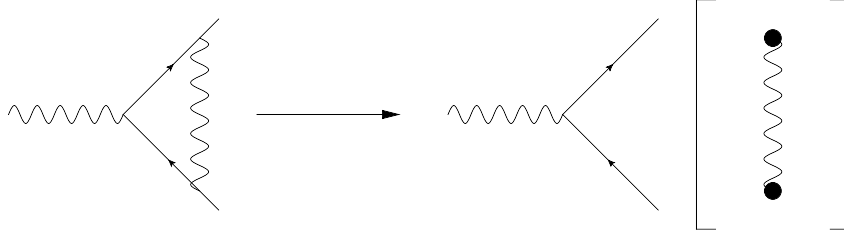


Figure 3: Pictorial depiction of the factorisation of the one loop graph of figure 2(b) in the soft photon limit, where \bullet denotes an eikonal Feynman rule.

The Dirac equations for the fermion and antifermion spinors ($\bar{u}(p) \not{p} = \not{p}v(p) = 0$) imply that the first terms of eqs. (7) and (8) vanish. Then eq. (6) becomes

$$\mathcal{A}_1 \rightarrow [\bar{u}(p)\gamma^\mu v(\bar{p})] \left(-\frac{p^\alpha}{p \cdot k} \right) \left(\frac{\bar{p}^\alpha}{\bar{p} \cdot k} \right) D_{\alpha\beta}(k). \quad (9)$$

We may note the following from this expression:

- The tree-level interaction \mathcal{A}_0 factors out, and is not IR divergent. Thus, this is an explicit example of the factorisation of soft physics from hard, which is embodied more generally by eq. (2). The essential reason for this factorisation is that a soft photon has an infinite Compton wavelength, and therefore cannot resolve the details of the hard interaction (which, by the uncertainty principle, takes place over relatively short distance scales).
- The emission of a soft photon from the fermion or anti-fermion line is described by the *eikonal Feynman rule*

$$\frac{p^\mu}{p \cdot k}, \quad (10)$$

where the sign is different on the two lines due to the fact that the momentum k is outgoing at one vertex, but incoming at the other. Here we have considered soft photon emission from fermion lines, but in fact the same Feynman rule would have resulted had we considered scalar or vector particles. The reason for this is again due to the large Compton wavelength of the soft photon, which cannot resolve the magnetic moment of the emitting particle, hence is insensitive to the spin.

- We can think of the factors multiplying the tree-level interaction \mathcal{A}_0 as a Feynman diagram by itself, albeit with effective Feynman rules. This is illustrated pictorially in figure 3, where we draw the one loop amplitude in the soft limit as the product of the tree level diagram with an effective Feynman diagram involving two eikonal Feynman rules joined by a photon propagator. The latter part is a *subdiagram* of the full amplitude which spans the hard external lines, and generates the IR singularities of the amplitude following the integration over the photon momentum k .

Having observed the factorisation of soft photon physics at the one loop level, the next step is to consider what happens when we add any number of soft photon emissions. At a given order $\mathcal{O}(\alpha^n)$ there are many different possibilities, two of which are shown in figure 4(a). Each diagram gives

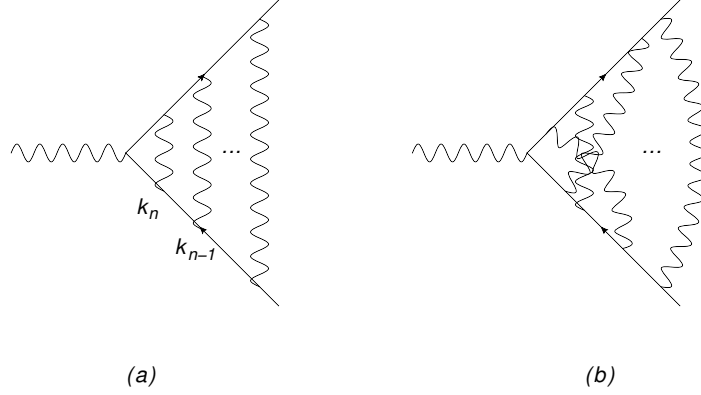


Figure 4: Two diagrams which contribute at $\mathcal{O}(\alpha^n)$, where in the left-hand diagram we label the momentum of the i^{th} gluon by k_i .

$$\left(\text{Soft diagrams at } \mathcal{O}(\alpha^n) \right) = \text{Tree-level diagram} \cdot \frac{1}{n!} \left[\text{Diagram with } n \text{ photon lines} \right]^n$$

Figure 5: Pictorial representation of the sum of all soft photon diagrams at $\mathcal{O}(\alpha^n)$, using the same notation as figure 3.

a somewhat complicated expression, as we will see in the following. However, a very simple result is obtained in the soft limit for the sum of all diagrams at $\mathcal{O}(\alpha^n)$, which is illustrated pictorially in figure 5. This shows that in the sum of all soft photon diagrams, the tree-level interaction \mathcal{A}_0 again factors out. The remainder is simply related to the one loop diagram raised to the power n , where the product is meant in the same sense as in figure 3. We may prove this result as follows.

Let us first consider the particular diagram shown in figure 4(a), consisting of n uncrossed photon exchanges. This is usually referred to as a *ladder diagram* in the literature. The expression for this diagram has the general form

$$\mathcal{A}_a^{(n)} = \bar{u}(p) Q^{\alpha_1 \dots \alpha_n} \gamma^\mu \bar{Q}^{\beta_1 \dots \beta_n} D_{\alpha_1 \beta_1}(k_1) \dots D_{\alpha_n \beta_n}(k_n), \quad (11)$$

where the tensors $Q^{\alpha_1 \dots \alpha_n}$ and $\bar{Q}^{\beta_1 \dots \beta_n}$ collect all factors from the fermion and anti-fermion lines respectively, and we have included the product of photon propagators such that the i^{th} photon has Lorentz indices α_i, β_i . Again, we do not explicitly show the integrals over the loop momenta k_i ,

and ignore coupling constants etc. The factors associated with the quark line are

$$\bar{u}(p)Q^{\alpha_1\dots\alpha_n} = \frac{\bar{u}(p)\gamma^{\alpha_1}(\not{p}-\not{k}_1)\gamma^{\alpha_2}(\not{p}-\not{k}_1-\not{k}_2)\dots\gamma^{\alpha_n}(\not{p}-\not{k}_1-\dots-\not{k}_n)}{(p-k_1)^2(p-k_1-k_2)^2\dots(p-k_1-k_2-\dots-k_n)^2}, \quad (12)$$

which in the soft limit of $k_i \rightarrow 0$ for each i becomes

$$\bar{u}(p)Q^{\alpha_1\dots\alpha_n} = \frac{\bar{u}(p)\gamma^{\alpha_1}\not{p}\gamma^{\alpha_2}\not{p}\dots\gamma^{\alpha_n}\not{p}}{[-2p\cdot k_1][-2p\cdot(k_1+k_2)][-2p\cdot(k_1+k_2+\dots+k_n)]}. \quad (13)$$

As in the case of one photon emission, one may anticommute the factors of \not{p} through the Dirac matrices, to act on the spinor $\bar{u}(p)$. All terms involving $\bar{u}(p)\not{p}$ vanish from the Dirac equation, leaving

$$\bar{u}(p)Q^{\alpha_1\dots\alpha_n} = \frac{\bar{u}(p)(-1)^n p_1^{\alpha_1}\dots p_n^{\alpha_n}}{p\cdot k_1 p\cdot(k_1+k_2) p\cdot(k_1+\dots+k_n)}. \quad (14)$$

Similarly for the factors on the anti-fermion line one finds

$$\bar{Q}^{\beta_1\dots\beta_n}v(\bar{p}) = \frac{\bar{p}^{\beta_1}\dots\bar{p}^{\beta_n}}{\bar{p}\cdot k_1 \bar{p}\cdot(k_1+k_2)\dots\bar{p}\cdot(k_1+\dots+k_n)}v(p), \quad (15)$$

such that the amplitude of eq. (11) becomes

$$\begin{aligned} \mathcal{A}_a^{(n)} = \mathcal{A}_0 \left\{ \frac{(-1)^n p^{\alpha_1}\dots p^{\alpha_n} \bar{p}^{\beta_1}\dots\bar{p}^{\beta_n}}{p\cdot k_1 p\cdot(k_1+k_2)\dots p\cdot(k_1+\dots+k_n) \bar{p}\cdot k_1 \bar{p}\cdot(k_1+k_2)\dots\bar{p}\cdot(k_1+\dots+k_n)} \right. \\ \left. \times D_{\alpha_1\beta_1}(k_1)\dots D_{\alpha_n\beta_n}(k_n) \right\}. \quad (16) \end{aligned}$$

Again we see that the tree-level interaction \mathcal{A}_0 has factored out, and clearly this will happen for any such soft photon diagram at arbitrary order. Note that the denominators in eq. (16) indicate a complicated dependence on the photon momenta k_i . These are coupled nontrivially along both the fermion and the anti-fermion line, so a given photon somehow knows about all other photons lying between itself and the final state hard particles. However, we have only considered one diagram at this order, and must now consider summing over all such diagrams.

This set of diagrams is illustrated for the $n = 3$ case in figure 6, where we see that there are six diagrams involving three photon emissions. We can think of obtaining this set by fixing the order of the photon emissions on the lower (anti-fermion) line, and summing over all permutations of emission orders on the upper (fermion) line. Thus, the total number of diagrams should be the same as the total number of permutations of three objects, which is $3! = 6$ as observed. Returning to the general case of n photon emissions, we may write the complete sum over all diagrams from eq. (16) as

$$\begin{aligned} \mathcal{A}_a^{(n)} = \mathcal{A}_0 \left\{ \frac{(-1)^n p^{\alpha_1}\dots p^{\alpha_n} \bar{p}^{\beta_1}\dots\bar{p}^{\beta_n}}{\bar{p}\cdot k_1 \bar{p}\cdot(k_1+k_2)\dots\bar{p}\cdot(k_1+\dots+k_n)} D_{\alpha_1\beta_1}(k_1)\dots D_{\alpha_n\beta_n}(k_n) \right. \\ \left. \times \sum_{\pi} \frac{1}{p\cdot k_{\pi_1} p\cdot(k_{\pi_1}+k_{\pi_2})\dots p\cdot(k_{\pi_1}+\dots+k_{\pi_n})} \right\}. \quad (17) \end{aligned}$$

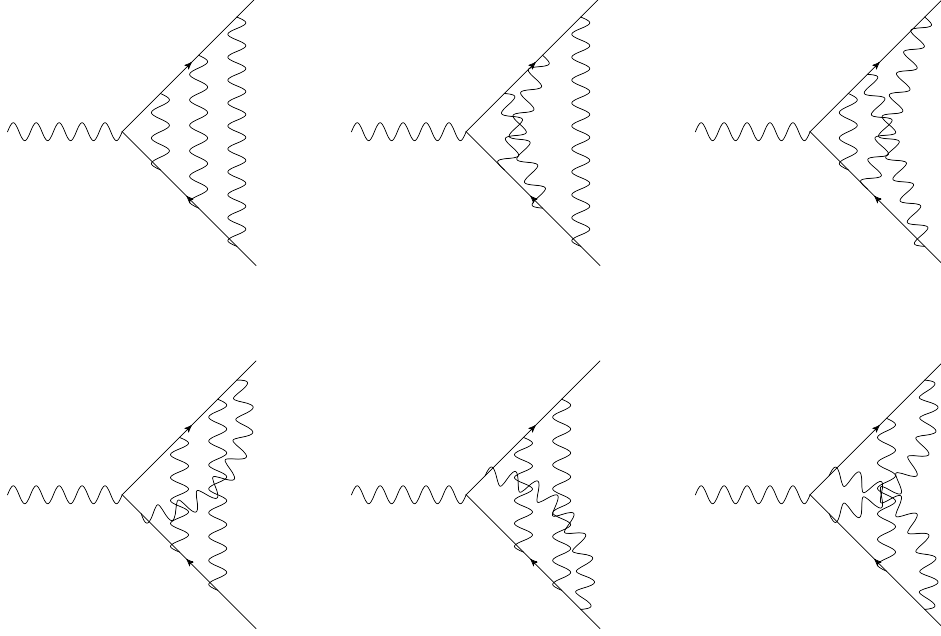


Figure 6: Complete set of diagrams involving three photon emissions at $\mathcal{O}(\alpha^3)$.

Here π labels a permutation of $(1, 2, \dots, n)$, such that this maps to $(\pi_1, \pi_2, \dots, \pi_n)$. The rather formidable looking formula of eq. (17) can be drastically simplified if we make use of the *eikonal identity*

$$\sum_{\pi} \frac{1}{p \cdot k_{\pi_1} p \cdot (k_{\pi_1} + k_{\pi_2}) \dots p \cdot (k_{\pi_1} + \dots + k_{\pi_n})} = \prod_i \frac{1}{p \cdot k_i}. \quad (18)$$

In order to make sense of this result, it is instructive to consider the case of $n = 2$, in which eq. (18) reduces to

$$\frac{1}{p \cdot k_1 p \cdot (k_1 + k_2)} + \frac{1}{p \cdot k_2 p \cdot (k_1 + k_2)} = \frac{p \cdot k_1 + p \cdot k_2}{p \cdot k_1 p \cdot k_2 p \cdot (k_1 + k_2)} = \frac{1}{p \cdot k_1 p \cdot k_2}, \quad (19)$$

which is indeed the stated result. We see that the eikonal identity is a sort of partial fraction identity, and the general result could be proven e.g. by induction from lower orders.

Problem 1. Show by explicit calculation that the eikonal identity works for the $n = 3$ case.

Substituting eq. (18) into eq. (17), the latter becomes

$$\mathcal{A}_a^{(n)} = \mathcal{A}_0 \left\{ \frac{(-1)^n p^{\alpha_1} \dots p^{\alpha_n} \bar{p}^{\beta_1} \dots \bar{p}^{\beta_n}}{\bar{p} \cdot k_1 \bar{p} \cdot (k_1 + k_2) \dots \bar{p} \cdot (k_1 + \dots + k_n)} D_{\alpha_1 \beta_1}(k_1) \dots D_{\alpha_n \beta_n}(k_n) \right. \\ \left. \times \prod_{i=1}^n \frac{1}{p \cdot k_i} \right\}. \quad (20)$$

This result is already a lot simpler than eq. (17) for one important reason: the photons on the upper line are now completely decoupled from each other. This is not true for the photons on the lower line. However, one may achieve this by exploiting the fact that all of the momenta k_i are dummy variables which are ultimately integrated over. Furthermore, the product of photon propagators contracted with the momentum factors is symmetric under interchange of any two momenta, subject to suitable relabelling of dummy Lorentz indices. Thus, by relabelling the integration variables one may replace the particular combination of photon momenta appearing in the first line of eq. (20) with any permutation of these momenta. That is, one may write

$$\begin{aligned} & \int d^d k_1 \dots \int d^d k_n \frac{1}{\bar{p} \cdot k_1 \bar{p} \cdot (k_1 + k_2) \dots \bar{p} \cdot (k_1 + \dots + k_n)} \\ &= \frac{1}{n!} \int d^d k_1 \dots \int d^d k_n \sum_{\pi} \frac{1}{\bar{p} \cdot k_{\pi_1} \bar{p} \cdot (k_{\pi_1} + k_{\pi_2}) \dots \bar{p} \cdot (k_{\pi_1} + \dots + k_{\pi_n})}. \end{aligned} \quad (21)$$

In the second line, we have used the fact that each term gives the same result (by relabelling dummy integration variables), and that there are $n!$ such permutations. Substituting this result into eq. (20) and tidying things up (again omitting the integrations over the momenta for brevity), one ultimately finds

$$\begin{aligned} \mathcal{A}^{(n)} &= \mathcal{A}_0 \frac{1}{n!} \prod_{i=1}^n \left(\frac{-p^{\alpha_i}}{p \cdot k_i} \right) \left(\frac{\bar{p}^{\beta_i}}{\bar{p} \cdot k_i} \right) D_{\alpha_i \beta_i}(k_i) \\ &= \mathcal{A}_0 \frac{1}{n!} \left[\left(\frac{-p^{\alpha}}{p \cdot k} \right) \left(\frac{\bar{p}^{\beta}}{\bar{p} \cdot k} \right) D_{\alpha \beta}(k) \right]^n, \end{aligned} \quad (22)$$

which is precisely the result expressed pictorially in figure 5, namely that the sum over all n photon graphs in the soft limit is simply related to the n^{th} power of the one loop graph.

The astute reader will have noticed that eq. (22) (which includes the leading order result) is the n^{th} term in the Taylor expansion of an exponential. Thus, one may explicitly compute the sum of all diagrams involving any number of single soft photon emissions, to all orders in perturbation theory! The result is

$$\mathcal{A} = \mathcal{A}_0 \exp \left[\int \frac{d^d k}{(2\pi)^d} \left(\frac{-p^{\alpha}}{p \cdot k} \right) \left(\frac{\bar{p}^{\beta}}{\bar{p} \cdot k} \right) D_{\alpha \beta}(k) \right], \quad (23)$$

where we have reinstated the integral over the gluon momentum. This result is shown using our pictorial notation in figure 7. In later sections, we will end up considering diagrams with many hard particles connected by soft gauge bosons. Thus, it is useful to redraw figure 7 so as to include the hard interaction in the exponent, as shown in figure 8. The purpose of this is simply to clearly display which lines the photon is emitted between - we *do not mean* that the hard interaction itself exponentiates.

We have now derived our first example of exponentiation. Some further comments:

- (i) The one loop graph in the exponent of eq. (23) has an IR divergence. Were we to explicitly expand the exponential, we would thus find that IR singularities at higher orders in the amplitude are related to singularities at lower orders.

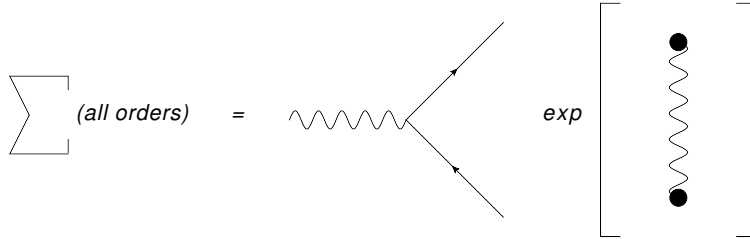


Figure 7: Pictorial representation of the exponentiation result of eq. (23).

$$A = A_0 \exp \left[\text{diagram} \right]$$

The diagram inside the square bracket shows a wavy line (photon) splitting into two straight lines (fermions). The upper straight line has a wavy line (soft photon) attached to it, with an arrow pointing away from the vertex, indicating emission from that particle.

Figure 8: Alternative drawing of figure 7, making clear which outgoing particles emit the soft photon.

- (ii) Here we considered only graphs with single photon emissions, finding that these are entirely given by the exponential of the one loop graph. In fact, this is not the whole story - soft photons could also connect off the external lines, via fermion bubbles. The complete result is then that the exponent contains all connected soft photon subgraphs, as depicted in figure 9. In principle one can prove this using a generalisation of the above method [65]. We will instead prove this result using alternative means in the following section.
- (iii) Above, we only considered two outgoing hard particles. However, the result can be extended to any number of external lines, where again the exponent contains all possible connected subgraphs which span the hard particle lines.
- (iv) Things are, unsurprisingly, more complicated in non-abelian gauge theories. Crucial to the above argument was that we could sum over all permutations of photon emissions, where these were weighted equally. This is no longer the case in e.g. QCD, where the emission vertices carry colour matrices \mathbf{T}^a which do not commute. Thus, an additional level of combinatoric complexity arises.
- (v) Things are not much more complicated in perturbative quantum gravity. This is a theory that shares features of QED and QCD. It is QED-like in that soft graviton emission vertices commute with each other (i.e. do not carry a non-commuting matrix-valued charge). It is QCD-like in that there are three and four graviton vertices, which mimic the corresponding gluon self-interactions in QCD. However, the charge in gravity is the 4-momentum of a particle. Thus, all multiple vertices between soft (zero momentum) gravitons vanish. A careful analysis also shows that diagrams in which gravitons couple to matter loops also vanish [27, 29]. Hence, IR divergences are given to all orders in quantum gravity purely from the exponentiation of the one-loop result, a property known as *one-loop exactness*. In other

$$A = A_0 \exp \left[\text{diagram 1} + \text{diagram 2} + \dots \right]$$

Figure 9: Complete result for abelian exponentiation, in which all possible connected soft photon subgraphs appear in the exponent.

words, the structure of IR divergences in quantum gravity is, remarkably, simpler than in QED!

In section 1, we defined a web as being a diagram which contributes to the exponent of the soft function. We have now seen our first examples of webs, and the results of this section can be compactly summarised as follows:

Webs in abelian gauge theories are connected subdiagrams.

At this point, we could leave the case of QED in favour of exploring non-abelian gauge theories. The traditional treatment of webs in the latter case proceeds by generalising the eikonal identity to take into account non-trivial colour structure. One may then explicitly solve for the structure of webs in scattering amplitudes which involve only two coloured external particles [66–68]². We choose not to follow such an approach here. Firstly, there is the lack of generality implied by the restriction to processes involving only two coloured particles (although three particles can also be treated straightforwardly using similar methods [69])³. Secondly, one may develop a more general approach for deriving exponentiation, which works for both abelian and non-abelian gauge theories, and any number of outgoing particles. In order to introduce this method, we will start by rederiving the results of abelian exponentiation. This is the subject of the following section.

3 The Path Integral Approach

In the previous section, we saw that the soft function itself has a Feynman diagram interpretation, where these diagrams consisted of effective Feynman rules for emission of soft gluons from hard outgoing particles. The propagators joining these vertices were the usual propagators arising from the action for the soft gauge field. Furthermore, these diagrams were *subdiagrams* in the full amplitude. That is, if one removes the hard interaction and the hard outgoing particle lines, what is left is the soft gluon diagram. This is illustrated in figure 10, for a scattering amplitude involving five external particle legs. In practice, as we saw at the end of the previous section, it is useful to also draw the external lines in the soft photon subdiagram, so as to indicate which external line a given soft photon was emitted from. This matters given that the hard momentum p^μ enters the

²For a pedagogical exposition, see [69].

³See also [70–72] for an examination of the general multileg case.

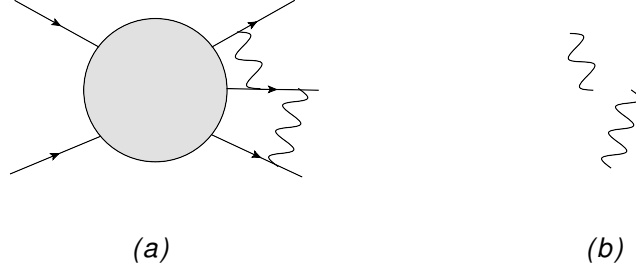


Figure 10: (a) An example scattering amplitude involving five external hard particles, and two soft photons; (b) soft photon subdiagram.

eikonal Feynman rule.

Given that Feynman diagrams exist purely for the soft subdiagrams, it follows that there must be a quantum field theory for the soft gauge field by itself, whose diagrams are the soft photon subdiagrams. One way of specifying a QFT is to write down its *generating functional*, from which all Feynman diagrams can be derived. Here we will simply write down the generating functional which generates soft photon subdiagrams (see [12] for a full derivation). It is given by ⁴

$$Z = \int \mathcal{D}A_\mu e^{iS[A_\mu]} \prod_{k=1}^L e^{i \int dx_k^\mu A_\mu(x_k)}, \quad (24)$$

where A_μ is the (soft) gauge field with action $S[A_\mu]$, and the product is over external particles, L in total. The exponential factors contain the space-time trajectory of the k^{th} particle, which is given by

$$x_k^\mu = n_k^\mu t, \quad (25)$$

where n_k^μ is a (constant) 4-vector proportional to the 4-momentum of the particle, p_k^μ . Note that we have taken each outgoing particle as having a zero initial position. Thus, all the hard particles originate from the origin, which corresponds to having shrunk the hard interaction which produces these particles to an infinitely small region of space-time. This is an approximation of course, but it turns out that corrections to this approximation are formally subleading, in that they involve additional powers of the emitted gluon momenta, which in the soft limit have been taken to zero. The physics of this approximation is that soft gluons, as discussed above, have an infinite Compton wavelength. Thus, they are not able to resolve the internal details of the hard interaction, which consequently appears pointlike.

Let us discuss the form of the generating functional of eq. (24). Firstly, there is a path integral over all possible configurations of the soft gauge field, where each is weighted by a phase factor involving the classical action. This is what one expects for the path integral representation of a quantum field theory. The additional factors (one for each external leg) are exponential, where the exponent is linear in the gauge field. This thus acts as a *source term* for the soft gauge field. In other words, vertices will be generated, which enable a soft photon to pop out of the vacuum. The

⁴Here we have absorbed a factor of the coupling constant into the gauge field.

form of the exponent tells us that each vertex is located in space-time along one of the external leg trajectories x_k^μ . We can see what the momentum space Feynman rule is for such a vertex by first rewriting the exponent of each external line factor as

$$\exp \left[i \int dx_k^\mu A_\mu \right] = \exp \left[i \int_0^\infty dt n_k^\mu A_\mu(x^\mu) \right], \quad (26)$$

where we have substituted the trajectory of eq. (25). Next, we may write the soft gauge field in terms of its Fourier transform using

$$A_\mu(x) = \int \frac{d^d k}{(2\pi)^d} \tilde{A}_\mu(k) e^{ik \cdot x}. \quad (27)$$

Substituting this into eq. (28), the exponent becomes

$$\begin{aligned} i \int_0^\infty dt n_k^\mu A_\mu(n_k^\mu t) &= \int \frac{d^d k}{(2\pi)^d} \tilde{A}_\mu(k) i \int_0^\infty dt n_k^\mu e^{i(k \cdot n_k)t} \\ &= \int \frac{d^d k}{(2\pi)^d} \tilde{A}_\mu(k) i n_k^\mu \left[\frac{e^{i(k \cdot n_k)t}}{ik \cdot n_k} \right]_0^\infty \\ &= \int \frac{d^d k}{(2\pi)^d} \tilde{A}_\mu(k) \left(-\frac{n_k^\mu}{n_k \cdot k} \right). \end{aligned} \quad (28)$$

Here we have been rather cavalier in dealing with the upper limit in the second line. A more careful treatment - including the Feynman $i\varepsilon$ prescription - gives the same result. By the usual procedure for reading Feynman rules from the exponent inside the path integral, the integrand of the momentum integral (represented by the term in brackets in the last line of eq. (28)) is the momentum space Feynman rule. Given that this is evidently invariant under rescalings of the vector $n_k^\mu \propto p_k^\mu$, we may replace this Feynman rule with ⁵

$$-\frac{p_k^\mu}{p_k \cdot k},$$

which is the correct Feynman rule for the emission of a soft photon from a hard external particle, as given in eq. (10).

Problem 2. For hard particles emitting soft gravitons (described by a spin two field $h_{\mu\nu}(x)$), the analogue of the external line factor of eq. (26) is ⁶

$$\exp \left[-i \frac{\kappa}{2} \int_0^\infty ds p^\mu p^\nu h_{\mu\nu}(sp) \right],$$

where p^μ is the momentum of the particle emitting the gravitons, s is a parameter such that $x^\mu = sp^\mu$, and $\kappa = \sqrt{16\pi G_N}$, where G_N is Newton's constant. Show that this leads to an effective momentum-space Feynman rule for graviton emission given by

$$\frac{\kappa p^\mu p^\nu}{2 p \cdot k}.$$

⁵The rescaling symmetry of the eikonal Feynman rules is actually broken when the Wilson lines are null - see e.g. [16] for a discussion. For our purposes, we can take the Wilson lines to be massive i.e. $p_k^2 \neq 0$.

The above discussion justifies why eq. (24) is the correct generating functional for soft photon subdiagrams. It generates the right Feynman rules for emission of soft photons from external lines. Furthermore, these will be joined by propagators, as generated by the action for the soft gauge field $S[A^\mu]$ ⁷. Thus, the diagrams generated by eq. (24) are indeed the soft photon diagrams we are after, which are in turn subdiagrams in the full amplitude.

There is another way to look at the external line factors in eq. (24), which is to notice that they are *Wilson line* operators. The general definition of such an operator is⁸

$$\Phi(\mathcal{C}) = \exp \left[i \int_{\mathcal{C}} dx^\mu A_\mu(x) \right], \quad (29)$$

where \mathcal{C} is some contour in space-time. Such operators transport gauge information from point to point in space-time, along the chosen path. What eq. (24) then generates is a vacuum expectation value of Wilson line operators, evaluated along the classical trajectories of the outgoing hard particles. This is in fact a restatement of an old result [5, 75], namely that IR singularities due to soft gluon emission from hard quarks or gluons can be described by dressing the hard particles by Wilson line operators. The physics behind this is as follows: if outgoing particles are emitting soft (zero-momentum) gluons, they do not recoil. Thus, they must follow their classical straight-line trajectories. They can, however, change by a phase. If this phase is to have the right gauge-transformation properties to be part of a scattering amplitude, it must be a Wilson line operator. Given that eq. (24) generates the soft function in the amplitude, another way to say the above is that the soft function is a vacuum expectation value of Wilson lines, or:

$$\mathcal{S} \sim \left\langle 0 \left| \prod_{k=1}^L \Phi_k \right| 0 \right\rangle, \quad (30)$$

where Φ_k is a Wilson line operator evaluated along the trajectory x_k of particle k . Indeed, this is usually taken as the definition of the soft function (see e.g. [16]).

Having introduced the generating functional for the soft gauge field theory, we now proceed to use this in order to rederive abelian exponentiation. To this aim, we introduce a crafty statistical physics approach, which is the subject of the following section.

3.1 The replica trick

In the previous section, we introduced a generating functional for a QFT for the soft gauge field A_μ , which generated soft photon subdiagrams. If we consider the simple case of QED with no propagating fermions (so that soft photon graphs contain no fermion bubbles), the path integral over A_μ in eq. (24) is Gaussian, and can be carried out exactly. This would lead immediately to abelian exponentiation, which we already encountered in section 2. In the more complicated cases of QCD and QED with fermion bubbles, it is no longer the case that the path integral in the generating functional can be performed exactly, and so we instead wish to introduce a method for deriving exponentiation of soft gauge boson diagrams which will be fully general. Specifically, we will use

⁷Note that we have been somewhat lax with our notation for this action, which also includes couplings to matter particles, so that fermion loops are generated in soft photon diagrams.

⁸As in the preceding discussion, we have here omitted a factor of the charge e of the emitting particle.

the *replica trick*, a technique borrowed from statistical physics (see e.g. [76]). We will see that this provides an elegant shortcut to exponentiation, which bypasses the nontrivial combinatorics (e.g. the eikonal identity) that we encountered in section 2.

The argument proceeds as follows. Instead of the field theory defined by eq. (24), let us instead consider a theory with N identical copies, or *replicas*, of the soft gauge field A_μ . We can label these replicas by $A_\mu^{(j)}$, where $1 \leq j \leq N$. Importantly, we take these replicas to be non-interacting. That is, a given replica does not interact with other replicas, so that the set of replica gauge fields is mutually independent.

By generalising eq. (24), the generating functional for the replicated theory is

$$Z_{\text{rep.}} = \int \mathcal{D}A_\mu^{(1)} \mathcal{D}A_\mu^{(2)} \dots \mathcal{D}A_\mu^{(N)} \exp \left[i \sum_{j=1}^N S[A_\mu^{(j)}] \right] \left[\prod_{k=1}^L e^{i \int dx_k \cdot A^{(1)}} \right] \dots \left[\prod_{k=1}^L e^{i \int dx_k \cdot A^{(N)}} \right]. \quad (31)$$

Here there is a path integral over all possible field configurations of each replica. The total action for the replicas is the sum of all the individual replica actions, as follows from the fact that the replicas are non-interacting. Furthermore, we now have a product of Wilson line factors for each external line, where this product occurs for each replica number from 1 to N . We can simplify eq. (31) by noting that the Wilson line factors in an abelian theory commute with each other, so that they can be combined into a single exponential to give

$$Z_{\text{rep.}} = \int \mathcal{D}A_\mu^{(1)} \mathcal{D}A_\mu^{(2)} \dots \mathcal{D}A_\mu^{(N)} \exp \left[i \sum_{j=1}^N S[A_\mu^{(j)}] \right] \prod_{k=1}^L \exp \left[i \sum_{j=1}^N \int dx_k \cdot A^{(j)} \right]. \quad (32)$$

What do the diagrams generated by this theory look like? Ignoring the replica index, the generating functional looks similar to the non-replicated theory, and so diagrams in the replicated theory have similar topologies to the original soft photon theory. However, we have to take account of the fact that each connected piece of a given diagram could have a different replica number. This is illustrated in figure 11, which shows three examples of soft photon diagrams, dressing the hard interaction of figure 2(a). The first example consists of two single soft photon emissions, each of which may potentially correspond to a different replica (shown using different colours in the figure). We can also think about this in terms of assigning indices i and j to each photon, where $1 \leq i, j \leq N$. In the second example, there are two disconnected pieces in the soft photon subdiagram: a single photon emission, and four photons connected to a fermion bubble. Each of the separate connected pieces is constrained to have a single replica number. This follows from the fact that the action for each replica, $S[A_\mu^{(j)}]$, implicitly includes coupling to fermion bubbles etc. Thus, replicas cannot mix via matter bubbles, which would ruin the fact that the replicas are independent. The third example in the figure shows two similar connected pieces arranged in a different way, so that there is some sort of non-trivial kinematic entanglement between the different parts of the photon subgraph. This does not affect the fact, however, that the two connected pieces are completely separate from each other if the external lines are removed (as defines the soft photon subgraph), and thus they may still have potentially different replica numbers.

The above discussion is perhaps rather unmotivated and mysterious! Let us now see how we can use the replicated theory to prove abelian exponentiation. Firstly, note that the replicated generating

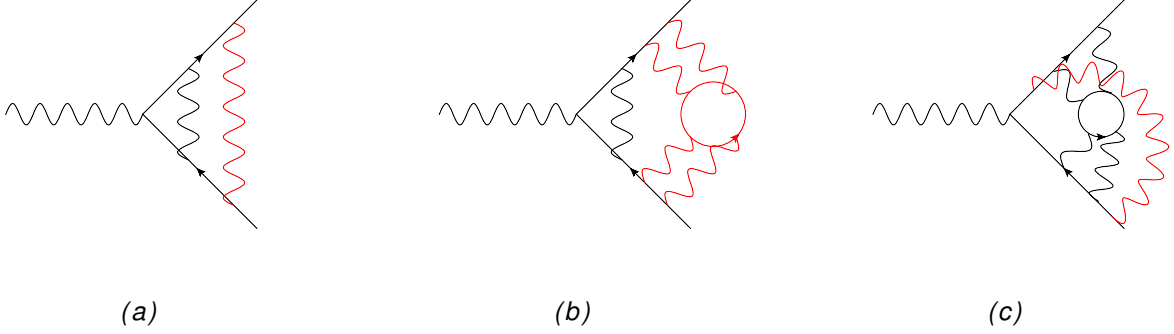


Figure 11: Examples of soft photon diagrams in the replicated theory of eq. (31). Different colours represent potentially different replica numbers.

functional of eq. (31) is related to the generating functional of the original theory, eq. (24), by the relation

$$Z_{\text{rep.}} = Z^N, \quad (33)$$

where as usual N is the total number of replicas. This follows from the fact that the replicas are non-interacting, so that one could choose to rewrite eq. (24) as a product of path integrals over each replica $A_\mu^{(i)}$ individually, thus making the structure of eq. (33) manifest. We may now Taylor expand this equation in N to give

$$Z_{\text{rep.}} = 1 + N \log Z + \mathcal{O}(N^2). \quad (34)$$

The left-hand side of this equation corresponds to a complete sum of Feynman diagrams in the replicated theory. These will, in general, be N dependent. Equation (34) then tells us that if we expand each Feynman diagram as a function of N , the coefficient of the $\mathcal{O}(N)$ piece contributes to the *logarithm* of Z (the generating functional of the original theory). Note that this argument does not depend on N being small - higher order terms in N contribute to higher powers of the logarithm of Z , which is irrelevant to our present logic.

It follows from the above discussion that if we find the $\mathcal{O}(N)$ part of all diagrams in the replicated theory (let us call this W for a given diagram), then the original generating functional is given by

$$Z = \exp \left[\sum_W W \right]. \quad (35)$$

Thus, Z has a manifestly exponential form. This is not a particularly impressive statement in general - it is always true that Z is the exponential of its own logarithm! However, what the replica trick gives us is an explicit procedure for determining the logarithm of Z ; in other words, for determining which diagrams exponentiate in the non-replicated theory.

To see how this works in this abelian case, consider for example the diagrams in figure 11(b) and 11(c). These both have two separate connected pieces in the soft photon part of the diagram, and each of these has a potentially different replica number. Given that there are N choices for the

first replica number and a further N for the second, it follows that diagrams with these topologies are $\mathcal{O}(N^2)$. Generalising this argument, a diagram with m separated connected pieces is $\mathcal{O}(N^m)$. Such diagrams, by the above argument, do not contribute to the exponent of Z , as they have no part which is linear in N . The only diagrams which are linear in N have $m = 1$ i.e. have only one connected piece. We have thus derived, from the replica trick, that connected diagrams exponentiate in the soft photon theory ⁹! All disconnected diagrams, such as those shown in figure 11(b) and (c), are obtained by the explicit exponentiation of lower order diagrams.

Recalling that Z generates subdiagrams in the full amplitude, namely those parts of the graph that contribute to the soft function, we have derived the result

$$\mathcal{S} = \exp[\text{Connected soft photon subgraphs}].$$

This is the abelian exponentiation result that we (partially) derived using the eikonal identity in the previous section. Some further comments are as follows:

- (i) The replica trick proof is much simpler than the eikonal identity approach. Essentially, what the replica trick does is to hide the tricky combinatorics associated with building up the exponential series. Using a traditional combinatoric approach would be even more complicated in non-Abelian theories, although it can of course be done [66–68, 70, 77].
- (ii) The replica trick works for any number of external lines. This will be particularly useful in the case of non-abelian gauge theories, in which results have traditionally been separated into the case of amplitudes with two coloured particles, and the general case of multiparton scattering.
- (iii) The above result shows that *all* connected diagrams exponentiate, including those containing fermion bubbles. We would have had to have proved this separately in the eikonal identity approach of section 2 (although admittedly this is a minor modification [65]).
- (iv) In the replica trick analysis, we explicitly used the fact that the Wilson line operators commute with each other, in order to combine their exponents into a single exponential factor for each external line. A similar result holds in quantum gravity, but not in non-abelian theories such as QCD. The latter have colour matrices associated with the emission of a soft gluon, which complicates the combinatorics of the path integral. In particular, the standard textbook result of exponentiation of connected diagrams does not hold for the field theory describing a soft gluon field (as we will see).

Having introduced the replica trick in this section, and described how this can be used to derive exponentiation properties, we are now ready to explore exponentiation in non-abelian theories.

4 Non-abelian exponentiation

In the previous section, we introduced the replica trick and showed how this can be used to derive abelian exponentiation. The main idea was that the $\mathcal{O}(N)$ part of Feynman diagrams in the

⁹This is in fact a special case of a general result in quantum field theory (which can be found in many textbooks, albeit often in an appendix), that connected diagrams exponentiate.

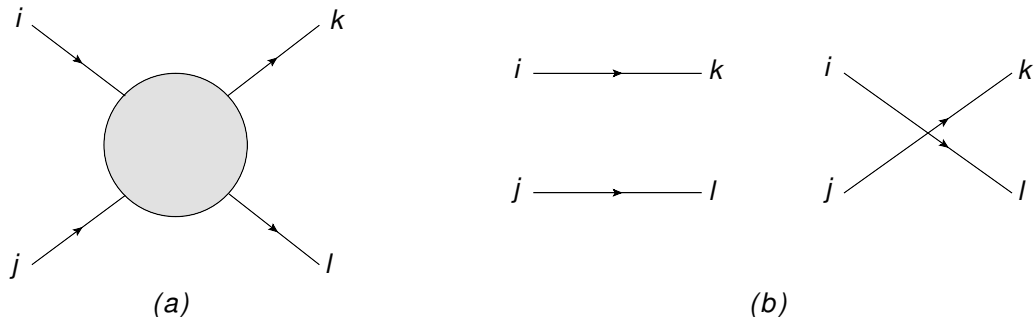


Figure 12: (a) Schematic depiction of $qq \rightarrow qq$ scattering, where the labels denote colour indices; (b) The two independent ways of joining up the colour flow.

replicated theory contributes to the exponent of the soft function in the non-replicated theory. Thus, one has an explicit procedure for calculating the exponent of the soft function directly. In non-abelian theories, the same overall procedure can be used, but leads to a much richer structure in the exponent that is still not fully understood.

Before examining non-abelian exponentiation in detail, it is worth making a few remarks regarding the existing literature on this subject. These are given in the following section, which can be skipped if necessary without affecting the flow of the argument from the previous section. However, what follows is useful for reasons of completeness, and for making contact with previous work on webs.

4.1 Two parton vs. multiparton scattering

Historically, non-abelian exponentiation was first considered in the case of scattering amplitudes involving only two coloured particles [66–68] (plus any number of colour singlet particles). Physical examples of these processes include Drell-Yan production of a vector boson, Higgs boson production via gluon fusion, deep inelastic scattering (in which an electron collides with a proton, which subsequently breaks up), and electron-positron annihilation into a quark-antiquark pair. In such processes, each external quark or gluon has a colour index. The special nature of amplitudes with only two coloured particles is that there is only one possible colour flow at the hard interaction vertex: the colour indices of the two quarks or gluons involved must join up with each other (by colour conservation). In a general multiparton scattering process, there are many colour indices joining up at the hard interaction vertex, and consequently there are many different ways of joining them up. Consider, for example, the case of $qq \rightarrow qq$ scattering, as shown in figure 12(a). Whatever is happening in the hard interaction, it remains true that there are only two ways of joining up the colour indices of the incoming and outgoing quarks. These are shown in figure 12(b). The scattering amplitude of this process will have four colour indices, as labelled in the figure 12(a). The two ways of joining the colour flow means that this amplitude must have the following form:

$$\mathcal{A}_{ijkl} = \mathcal{A}_1 \delta_{ik} \delta_{jl} + \mathcal{A}_2 \delta_{il} \delta_{jk}, \quad (36)$$

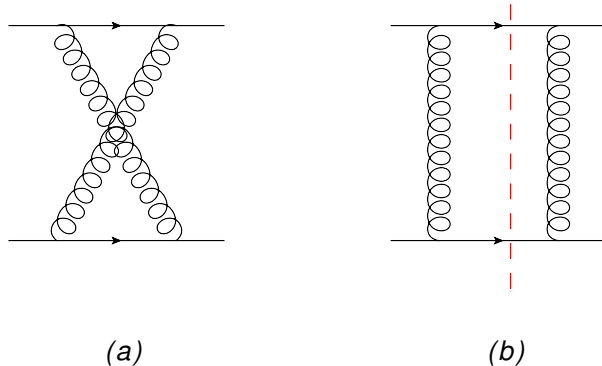


Figure 13: Examples of: (a) a two-eikonal line irreducible diagram; (b) a reducible diagram (the red line separates the two connected pieces).

where δ_{ij} is the Kronecker delta symbol, and $\{\mathcal{A}_i\}$ are kinematic coefficients which are independent of the colour index structure. We may rewrite this equation as

$$\mathcal{A} = \sum_I \mathcal{A}_I c_I, \quad (37)$$

where $I = 1, 2$ and the *colour tensors* $\{c_I\}$ are defined via

$$c_1 = \delta_{ik}\delta_{jl}, \quad c_2 = \delta_{il}\delta_{jk}. \quad (38)$$

In other scattering amplitudes, there are more ways of joining up the colour flow in general. However, amplitudes still have the generic form of eq. (37), with an appropriate set of colour tensors. These are not uniquely defined - any basis obtained via a linear transformation will do. Having chosen a basis, we can work with the components of the amplitude \mathcal{A}_I , and we see that amplitudes are *vectors in colour-flow space*. The soft function contains gluons which transfer colour from one external line to another in general. Thus, it mixes the various colour flows present in the hard interaction, and is matrix-valued in colour space. How such matrices act on the colour structure of the hard interaction is an interesting problem by itself - see e.g. refs. [78, 79].

Having introduced the above terminology, we can see why soft gluon emission in the case of two hard external lines is simpler in general than the multiline case. In the two line case, there is only one colour tensor (δ_{ij} , where i and j are the colour indices of the two external lines). The soft function is then a 1×1 matrix, and different contributions to the soft function commute with each other. This is in contrast to the general case of multiparton scattering, in which the soft function is a non-commuting object in colour flow space, and has implications for the structure of the exponent of the soft function. It turns out that in the two-line case, one can classify which diagrams appear to all orders in perturbation theory using a simple topological criterion, namely that they are *two-eikonal line irreducible*. This means that one cannot disconnect a given diagram by drawing a single line through both external lines, and an example is given in figure 13. Also shown is an example of a reducible diagram. In this case, figure 13(b) would not enter the exponent of the soft function, whereas 13(a) would. Recall that diagrams such as the latter were not present in the exponent in the

abelian case, so that even in the two-line case QCD is already much more complicated than QED ¹⁰.

Problem 3. Draw all irreducible diagrams at 3 loop order.

The above results for the two line case were derived in [66–68], and indeed it was a particular way of drawing two-eikonal line irreducible diagrams in those papers that first led to the term *web*. We will not present the derivation of this result here. It proceeds via a generalisation of the eikonal identity of eq. (18), which takes account of the fact that successive gluon emissions are non-commuting (for a recent presentation, see [45]). Rather, our aim is to present a formalism for non-abelian exponentiation, which is set up for the general case of multiparton scattering. The special properties of two-line scattering will then emerge as a special case. The following sections are based heavily on [77], but note that multiline webs have also been considered from a different point of view in [70]. For a discussion of how these two approaches are related, see appendix A of [80]. More recently, another approach has also appeared [71, 72].

4.2 The replica trick in a non-abelian theory

We now return to elucidating the structure of non-abelian exponentiation. In the abelian case of section 3, we used the replica trick to elegantly derive the exponentiation structure of the soft function, namely that connected soft photon subdiagrams enter the exponent. This strongly suggests that we should use the replica trick also in the non-abelian case. Let us then try this and see what happens.

First we need to write down the generating functional for the soft gluon theory, whose diagrams are the soft gluon subdiagrams of a non-abelian scattering amplitude. This is a straightforward generalisation of eq. (24), and the result is

$$Z = \int \mathcal{D}A_\mu e^{iS[A_\mu]} \prod_{k=1}^L \mathcal{P} e^{i \int dx_k^\mu A_\mu^k}. \quad (39)$$

This has a path integral over the soft gluon field, with a weighting factor containing the classical action. For ease of notation we use the same symbol $S[A_\mu]$ as in the QED case. However, the non-abelian action will contain three and four gluon vertices etc. in addition to the propagator and couplings to matter bubbles. Each external line, as before, has a Wilson line operator associated with it. This is similar to the QED Wilson line, except for the fact that the gauge field $A_\mu^k = A_\mu^a \mathbf{T}_k^a$ is matrix-valued, where \mathbf{T}_k is a colour matrix acting on the partonic colour indices of the k^{th} line. We do not write these colour indices explicitly in eq. (39), but we do add an index k to the soft gauge field to remind us that this lives in the colour index space of the k^{th} parton line. Given that the exponent of the Wilson line operator is matrix-valued, the exponential itself is ambiguous. Upon carrying out a Taylor expansion, it is not clear how to order the colour matrices in the correct fashion. This is corrected by the operator \mathcal{P} in eq. (39), which stands for *path ordering*. This operator is defined such that, in a given term in the expansion of the exponential, the colour matrices are ordered along the line according to the sequential ordering of gluon emissions. Parametrising the contour of a given line according to eq. (25), for example, this means that the colour matrices will

¹⁰This is only one complication of course. There are also soft gluon graphs in QCD which contain three and four gluon vertices, which do not exist in QED.

be ordered according to the order of the t values at which gluons are emitted. This is a somewhat subtle point that is absent in the case of an abelian gauge theory, where no non-commuting charges appear.

Applying the replica trick, one may consider the theory

$$Z_{\text{rep.}} = \int \mathcal{D}A_\mu^{(1)} \dots \mathcal{D}A_\mu^{(N)} \exp \left[i \sum_{j=1}^N S[A_\mu^{(j)}] \right] \times \left[\prod_{k=1}^L \mathcal{P} \exp \left(i \int dx_k^\mu A_\mu^{k(1)} \right) \right] \dots \left[\prod_{k=1}^L \mathcal{P} \exp \left(i \int dx_k^\mu A_\mu^{k(N)} \right) \right], \quad (40)$$

where we have again taken N independent (mutually non-interacting) copies of the gauge field. At this point in the abelian case, we collected together all Wilson line exponents to make a single exponential. We cannot do that in this case, due to the fact that the exponents of the Wilson line factors do not commute, if these act on the same external line. We can, however, commute Wilson line operators which act on *different* external lines. These have completely different colour indices, so that matrices on different lines commute simply by not living in the same colour algebra. This allows us to gather together the contributions from each external line separately in eq. (40), to get

$$Z_{\text{rep.}} = \int \mathcal{D}A_\mu^{(1)} \dots \mathcal{D}A_\mu^{(N)} \exp \left[i \sum_{j=1}^N S[A_\mu^{(j)}] \right] \prod_{k=1}^L \left[\prod_{j=1}^N \mathcal{P} \exp \left(i \int dx_k^\mu A_\mu^{k(j)} \right) \right]. \quad (41)$$

To recap, the first product in this formula is over all external lines. Then, each external line factor has a product of Wilson line operators acting on it, one for each replica. Furthermore, the replica number in this product increases from left to right, from 1 to N .

We cannot immediately read off the Feynman diagrams for the soft gauge field from eq. (41), as this contains a product of path-ordered exponentials for each external line. Were we inclined to rewrite this as a single path-ordered exponential, we would then be able to analyse the diagrams in more detail, by analogy with the case of the original theory. In general combining a number of exponentials involving non-commuting objects involves multiple applications of the Baker-Campbell-Hausdorff formula (see e.g. refs. [71,72,81] for approaches to exponentiation that build on this idea). However, we can circumvent this in a crafty way by exploiting the fact, mentioned above, that the replica number increases sequentially from 1 to N in the product of Wilson line operators associated with each external line. Thus, one may write this product as

$$\prod_{j=1}^N \mathcal{P} \exp \left(i \int dx_k^\mu A_\mu^{k(j)} \right) = \mathcal{R} \mathcal{P} \exp \left[i \sum_{i=1}^N \int dx_k^\mu A_\mu^{k(i)} \right]. \quad (42)$$

Here \mathcal{R} is a *replica-ordering operator*. Given a product of colour matrices on a given line, it ensures that the replica number increases along the line. We can define its action more formally by considering two colour matrices acting on line k . Denoting by $\mathbf{T}_k^{(i)}$ a colour matrix acting on line k and associated with a gluon with replica number i , one has

$$\mathcal{R} \left[\mathbf{T}_k^{(i)} \mathbf{T}_k^{(j)} \right] = \begin{cases} \mathbf{T}_k^{(i)} \mathbf{T}_k^{(j)} & i \leq j \\ \mathbf{T}_k^{(j)} \mathbf{T}_k^{(i)} & i > j \end{cases}. \quad (43)$$

That is, \mathcal{R} does nothing if the replica numbers associated with colour matrices are already increasing (or the same) along a given line, but reorders them if this is not the case. It is straightforward to generalise this definition to higher numbers of matrices. The \mathcal{R} operator then acts on each term in the expansion of the exponential on the right-hand side of eq. (42), and reorders the colour matrices such that the replica numbers in each term are in increasing order. Then the right-hand side agrees with the expansion of the multiple exponentials on the left-hand side which, if carried out, will have the replica numbers similarly ordered in every term. Note that the notation of eq. (42) implies that one first path orders (according to \mathcal{P}), and then replica orders (according to \mathcal{R}). In cases where these orderings are different \mathcal{R} overrides \mathcal{P} .

Substituting eq. (42) into eq. (41), we may rewrite the latter as

$$Z_{\text{rep.}} = \int \mathcal{D}A_{\mu}^{(1)} \dots \mathcal{D}A_{\mu}^{(N)} \exp \left[i \sum_{j=1}^N S[A_{\mu}^{(j)}] \right] \mathcal{R} \prod_{k=1}^L \left[\mathcal{P} \exp \left(i \sum_{j=1}^N \int dx_k^{\mu} A_{\mu}^{k(j)} \right) \right]. \quad (44)$$

Here, to simplify notation, we have defined an overall replica-ordering operator \mathcal{R} which is understood to act appropriately on each line k . Note that this now looks more similar to the QED case of eq. (32), apart from the colour-specific details (which are also present in the non-replicated QCD theory), and also the presence of the \mathcal{R} operator.

Consider now a particular soft gluon diagram D with a given topology. In the original (non-replicated) theory, this has the general form

$$\mathcal{F}(D)C(D),$$

where $C(D)$ is the colour factor of the graph (collecting all the soft gluon colour matrices on each external line), and $\mathcal{F}(D)$ contains all the kinematic dependence. In the replicated theory, the same diagram topology will have the similar form

$$\mathcal{F}(D)\hat{C}(D),$$

where $\mathcal{F}(D)$ is the same as in the original theory (as in the QED case, the kinematics of a given diagram does not care about the assignment of the replica numbers). However, the colour factor $\hat{C}(D)$ is *not the same* as in the original theory. Firstly, it depends on the number of replicas N . Secondly, colour factors are different in the replicated theory due to the fact that colour matrices, which obey path ordering only in the original theory, get reordered by the \mathcal{R} operator. The details of this reordering depend on the particular assignment of replica numbers in a given graph. To find the total colour factor in the replicated theory, one must also sum over the total number of replica assignments. The whole procedure is perhaps best illustrated by example.

Consider the two diagrams at two-loop order shown in figure 14. Here we have considered an amplitude with four external lines, and shrunk the hard interaction to a point. In the replicated theory, the two diagrams in the figure give contributions to the (replicated) amplitude

$$\mathcal{A}_a = \mathcal{F}(a)\hat{C}(a), \quad \mathcal{A}_b = \mathcal{F}(b)\hat{C}(b) \quad (45)$$

respectively. To find the total colour factor of diagram (a), one must consider all possible assignments of replica number i and j , as these will potentially contribute different amounts to the total,

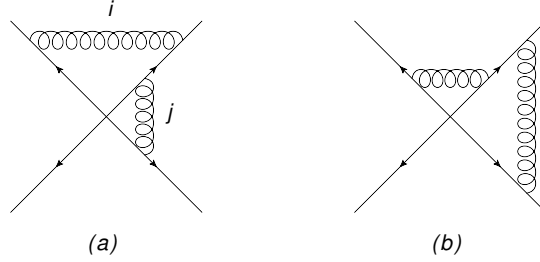


Figure 14: Example two-loop diagrams, where i and j denote replica numbers.

i, j	Replica-ordered colour factor	Multiplicity
$i = j$	$C(a)$	N
$i < j$	$C(b)$	$N(N - 1)/2$
$i > j$	$C(a)$	$N(N - 1)/2$

Table 1: Replica trick analysis of the diagrams of figure 14, as described in the text.

depending on the action of the replica ordering operator \mathcal{R} . Given that the action of this operator only depends upon whether replica indices are greater or less than each other (or the same), we need only consider three cases: $i = j$, $i < j$ and $i > j$. These are given in the first column of table 1, and the third column gives the total number of replica number assignments corresponding to each hierarchy of i and j . In the second column, we note the N -independent part of the contribution to the colour factor for each diagram. Considering first the case of $i = j$, this is simply the colour factor $C(a)$ of (a) in the original theory, as no replica reordering takes place if the replica indices are the same. If $i < j$, the gluons are not ordered in terms of increasing replica number on the upper right-hand line (where, according to the arrows to designate our choice of momentum flow, we are taking the direction of the Wilson line as increasing away from the hard interaction vertex). Then the colour matrices get reordered, which produces the conventional colour factor $C(b)$ of diagram (b). This is the reason why we have had to consider two diagrams at once - they mix with each other due to the \mathcal{R} operator. Finally, we must consider the case $i > j$. In this case the replica ordering constraint is already satisfied, and thus the N -independent part of the contribution to the colour factor is $C(a)$.

Putting things together, the total colour factor in the replicated theory is

$$\begin{aligned}
 \hat{C}(a) &= NC(a) + \frac{N(N-1)}{2} [C(a) + C(b)] \\
 &= N \left[\frac{C(a) - C(b)}{2} \right] + \mathcal{O}(N^2).
 \end{aligned}
 \tag{46}$$

Here we have formed the total by multiplying together the results of the second and third columns in table 1, and summing these up. In the second line we have taken the $\mathcal{O}(N)$ part of the colour factor, anticipating that this will be relevant in what follows.

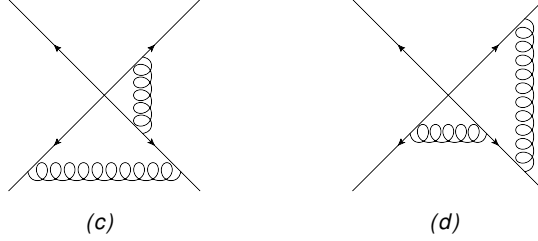


Figure 15: Diagrams considered in problem 4.

One may carry out a similar analysis for diagram (b) in figure 14, and the total colour factor in the replicated theory is found to be

$$\hat{C}(b) = N \left[\frac{C(b) - C(a)}{2} \right] + \mathcal{O}(N^2). \quad (47)$$

We may now use the replica trick argument from section 3, which said that the contribution of a given diagram D to the exponent of the generating functional in the non-replicated theory is given by the $\mathcal{O}(N)$ part of this diagram in the replicated theory. Thus, we see that both diagrams (a) and (b) contribute to the exponent of the soft function in the original theory, and they do so in the combination (taking the coefficients of the $\mathcal{O}(N)$ terms in eq. (46, 47))

$$\left(\frac{C(a) - C(b)}{2} \right) \mathcal{F}(a) + \left(\frac{C(b) - C(a)}{2} \right) \mathcal{F}(b). \quad (48)$$

Note that this can be rewritten in the matrix form

$$\begin{pmatrix} \mathcal{F}(a) \\ \mathcal{F}(b) \end{pmatrix}^T \frac{1}{2} \begin{pmatrix} 1 & -1 \\ -1 & 1 \end{pmatrix} \begin{pmatrix} C(a) \\ C(b) \end{pmatrix}. \quad (49)$$

This is an interesting structure, as the vectors on the left and right-hand side (defined in the space of diagrams) involve properties of the original theory, as they should now that we have returned from the replicated theory. The matrix in the middle consists of constant numbers, and describes a mixing between the colour and kinematic degrees of freedom of soft gluon diagrams in the exponent of the soft function. This structure is in fact entirely general, as we describe in the following section.

Problem 4. Without detailed calculation, write down the contribution to the soft gluon exponent of the diagrams in figure 15.

4.3 General structure of multiparton webs

In the previous section, we examined a particular set of diagrams that mix under the action of the \mathcal{R} operator. Both diagrams were found to contribute to the exponent of the soft function, but with a mixing matrix that entangles the colour and kinematic degrees of freedom. To see how this works in general, note first that the two diagrams of figure 14 are related by gluon permutations on the external lines. In this simple case, there is only one non-trivial permutation possible, on the upper right-hand line. Furthermore, this is a closed set: acting with more permutations will not

generate any additional diagrams. In general, given a diagram D involving arbitrary numbers of gluon attachments on arbitrary external lines (where these gluons may also be connected away from the external lines by fermion bubbles or multiple gluon vertices), we can always form such a closed set of diagrams related by gluon permutation operations. A further example is given in figure 16. It is clear that a given diagram can only mix with diagrams from the closed set to which it belongs. This is because the source of the mixing is the \mathcal{R} operator in the replicated theory, which is itself a form of gluon permutation operator, transforming between diagrams in such a closed set.

Now let W denote such a closed set. A given diagram $D \in W$ has a total colour factor $\hat{C}(D)$ in the replicated theory. This gives a contribution to the soft function in the original theory a quantity

$$\sum_D \mathcal{F}(D) \tilde{C}(D),$$

where we define $\tilde{C}(D)$ to be the coefficient of the $\mathcal{O}(N)$ part of $\hat{C}(D)$. This is the part of the colour factor in the replicated theory that contributes to the exponent of the soft function in the original theory. For this reason, $\tilde{C}(D)$ is referred to as the *exponentiated colour factor* (ECF) of diagram D [77]. In general, $\tilde{C}(D)$ will be a linear superposition of the original colour factors $C(D)$ (this superposition can in principle be found by applying the replica trick algorithm as outlined in the two loop example). Thus, one may write

$$\tilde{C}(D) = \sum_{D'} R_{DD'} C(D') \quad (50)$$

for some constants $R_{DD'}$. Let us now call the set of closed diagrams W a *web*, and $R_{DD'}$ elements of a *web mixing matrix*. This can be summarised as follows:

In non-abelian theories, webs are closed sets of diagrams related by gluon permutations on the external lines. Each web is described by a web mixing matrix, which encodes how colour and kinematic degrees of freedom mix in the exponent of the soft function.

It is perhaps clear that we want to consider a closed set of diagrams in some sense as a single web, given that these diagrams are mutually entangled. In fact, the motivation to call such sets webs goes further than this, as we will see in section 5. The general structure of the soft function in multiparton scattering can then be written schematically as

$$\mathcal{S} = \exp \left[\sum_W \sum_{D, D'} \mathcal{F}(D) R_{DD'}^{(W)} C(D') \right], \quad (51)$$

where the first sum is over all possible webs W with mixing matrices $R_{DD'}^{(W)}$, and the additional sums are over the diagrams in each web.

It is clear, then, that the general study of webs in multiparton scattering is dominated by the study of web mixing matrices. These encode a potentially huge amount of physics! Namely, web mixing matrices encode how colour and kinematic information is entangled to all orders in perturbation theory, and the hope is that significant insights into the physics of non-abelian gauge theories can be obtained by studying web mixing matrices.

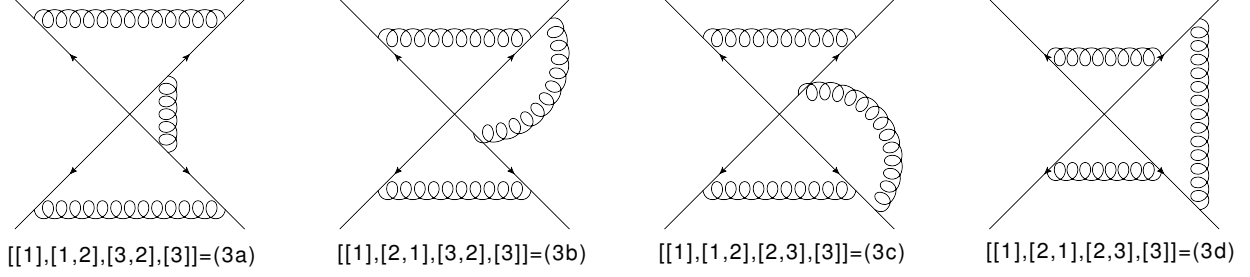


Figure 16: An example of a closed set of diagrams at three loop order.

i, j, k	Replica-ordered colour factor	Multiplicity
$i = j = k$	$C(3a)$	N
$i = j, k > i$	$C(3a)$	$N(N - 1)/2$
$i = j, k < i$	$C(3c)$	$N(N - 1)/2$
$i = k, j > i$	$C(3d)$	$N(N - 1)/2$
$i = k, j < i$	$C(3a)$	$N(N - 1)/2$
$j = k, i > j$	$C(3a)$	$N(N - 1)/2$
$j = k, i < j$	$C(3b)$	$N(N - 1)/2$
$i < j < k$	$C(3b)$	$N(N - 1)(N - 2)/6$
$i < k < j$	$C(3d)$	$N(N - 1)(N - 2)/6$
$j < i < k$	$C(3a)$	$N(N - 1)(N - 2)/6$
$j < k < i$	$C(3a)$	$N(N - 1)(N - 2)/6$
$k < i < j$	$C(3d)$	$N(N - 1)(N - 2)/6$
$k < j < i$	$C(3c)$	$N(N - 1)(N - 2)/6$

Table 2: Replica trick analysis for diagram (3a), as shown in figure 16. The replica indices i, j and k label the gluons on the upper, right-hand and lower parts of the diagram respectively.

4.4 A three loop example

In order to clarify the above statements, it is useful to consider a three loop example of applying the replica trick algorithm, to complement the two loop example from earlier. Consider the set of diagrams shown in figure 16, and let us calculate the exponentiated colour factor \tilde{C} of the diagram labelled (3a) in the figure. As in the two loop case, we must consider all possible assignments of replica numbers. Labelling the upper, right-hand and lower gluons with replica numbers i, j and k respectively, we must thus consider all possible hierarchies of i, j and k . These are given in table 2, which may be compared to the two loop example of table 1. As in the previous example, for each hierarchy of replica numbers, the N -independent part of the contribution to the total colour factor $\tilde{C}(3a)$ is found by applying the \mathcal{R} operation to the diagram, and matching the result to one of the other diagrams in the web. One must then multiply each result by the number of distinct replica number assignments that are consistent with the given hierarchy. These multiplicities are given in

the third column of table 2. The total colour factor in the replicated theory is then found to be

$$\begin{aligned}\hat{C}(3a) &= NC(3a) + \frac{N(N-1)}{2} [3C(3a) + C(3b) + C(3c) + C(3d)] \\ &\quad + \frac{N(N-1)(N-2)}{6} [2C(3a) + 2C(3d) + C(3b) + C(3c)].\end{aligned}\tag{52}$$

The exponentiated colour factor in the original theory is the coefficient of the $\mathcal{O}(N)$ part of this, which is

$$\begin{aligned}\tilde{C}(3a) &= C(3a) \left[1 - \frac{3}{2} + \frac{2}{6}\right] + C(3b) \left[-\frac{1}{2} + \frac{1}{6}\right] + C(3c) \left[-\frac{1}{2} + \frac{1}{6}\right] + C(3d) \left[-\frac{1}{2} + \frac{2}{6}\right] \\ &= \frac{1}{6} [C(3a) - C(3b) - C(3c) + C(3d)].\end{aligned}\tag{53}$$

From the definition of the web mixing matrix of eq. (50), this means that the first row of the web mixing matrix is $\frac{1}{6}(1, -1, -1, 1)$. In fact, the full matrix turns out to be [77]

$$R_{DD'} = \frac{1}{6} \begin{pmatrix} 1 & -1 & -1 & 1 \\ -2 & 2 & 2 & -2 \\ -2 & 2 & 2 & -2 \\ 1 & -1 & -1 & 1 \end{pmatrix}.\tag{54}$$

Problem 5. Verify this result by calculating the remaining rows of the matrix.

As the above problem demonstrates, calculation of web mixing matrices in any particular case is straightforward, but tedious. The algorithm can be - and indeed has been - automated. Many more examples of web mixing matrices can be found in [77, 82], and were obtained by computer.

4.5 General properties of web mixing matrices

We have now seen something of the general structure of multiparton webs, and in particular the fact that colour and kinematic parts of soft gluon diagrams mix according to web mixing matrices. We have seen examples of how to calculate these matrices in particular examples. Note in particular that this is a purely combinatoric exercise. This suggests, broadly speaking, two different ways to investigate the further properties of webs:

1. One may surmise the general structure of web mixing matrices by studying the *physics* of soft gluon graphs (e.g. the known properties of colour factors when the number of colours becomes large, or the need for infrared singularities to be consistent with renormalisation of the vertex at which all the external lines meet).
2. One may study general properties of web mixing matrices using *pure mathematics*, namely the combinatorics underlying the replica trick algorithm. The hope is then that established properties of the web mixing matrices can be translated into (previously unknown) physics.

Both of these are currently under investigation, and here we give a taste of some general features of web mixing matrices that have so far been established.

Firstly, we know that web mixing matrices have *zero sum rows*. That is, any mixing matrix satisfies

$$\sum_{D'} R_{DD'} = 0, \quad (55)$$

where the sum is over any row (labelled by D). One may verify this for the two examples given above in eqs. (49) and (54). This result means that one may redefine the ECF of all diagrams in a web by a common constant. Another way of looking at this is that the contribution to the colour factor of a given diagram which is completely symmetric under interchanges of diagrams in the web does not enter the exponent of the soft function. The zero sum row rule has also been extended in [80], where it is shown that certain subrows also sum to zero, corresponding to subsets of the web corresponding to planar and non-planar diagrams. Furthermore, a similar sum rule involving columns has been observed, involving extra weight factors [82].

Secondly, all web mixing matrices are *idempotent*, i.e.

$$\sum_E R_{DE} R_{ED'} = R_{DD'}. \quad (56)$$

This means that web mixing matrices are *projection operators*, having eigenvalues 0 and 1 (each with some multiplicity). These properties are crucial to the cancellation of infrared singularities in the exponent of the soft function, as has been explored in [55, 56, 82].

Both of the above properties have been proven to be completely general, including webs whose diagrams contain three and four gluon vertices [80]. The proof of the idempotence property involves applying the replica trick twice in succession, and arguing that this is equivalent to applying it once (i.e. replicating a theory M then N times is equivalent to replicating it MN times). The proof of the zero sum row property uses results from enumerative combinatorics, in particular the counting of partitions of sets via Stirling numbers of the second kind.

Recently, both the mathematics and physics behind web mixing matrices have been made clearer. In ref. [83], the combinatorics of mixing matrices was related to that of partially ordered sets, or *posets*. As the name suggests, a poset is a set of objects X endowed with an ordering operation \leq possessing the following properties:

1. *Reflexivity*. If $x \in X$ then $x \leq x$.
2. *Antisymmetry*. If $x \leq y$ and $y \leq x$ then $x = y$.
3. *Transitivity*. If $x \leq y$ and $y \leq z$, $x \leq z$.

This ordering operation applies to pairs of elements in the set X , but such that not all pairs are necessarily ordered with respect to each other (hence the “partially” in “partially ordered set”). The relation to web diagrams is as follows: every web diagram D can be identified with a poset. The elements of the poset are the various irreducible subdiagrams that occur in the diagram D . The ordering operation \leq is defined as follows: given two irreducible subdiagrams x and y , $x \leq y$ if x lies closer to the origin than y , in the sense that one cannot pull y into the origin without also pulling in x . As an example, consider the diagram shown in figure 17(a). In this diagram,

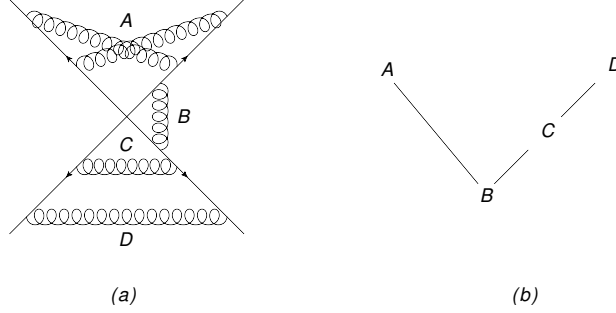


Figure 17: (a) Example web diagram; (b) Hasse diagram corresponding to the poset generated by the diagram in (a).

the two gluons labelled A form an irreducible subdiagram: the fact that they are crossed means that one cannot shrink either gluon to the origin independently of the other one. The single gluon exchanges labelled B , C and D are also irreducible subdiagrams. Then the structure of the diagram is encoded by the information that B must be shrunk before A , C or D , and C must be shrunk before D . This corresponds to the *Hasse diagram* shown in figure 17(b): a diagram whose vertices represent the elements of the poset, and whose edges denote an ordering between two elements.

Problem 6. Draw the Hasse diagrams for the web of figure 16, and hence show that these correspond to a (possibly kinked) chain of linked vertices.

The language of posets and Hasse diagrams is a powerful one. Reference [83] uses it to prove a number of general results, including results for the rank of the mixing matrix for three given families of web, for any number of gluons. Reference [84] carries this even further. For two particular web families, solutions are given for the web mixing matrix for any number of gluons. This hints at the possibility that the combinatorics of web mixing matrices could be completely classified, and that it would be possible to go straight from web diagrams to the mixing matrix, without having to apply the replica trick algorithm.

The physical content of web mixing matrices has been clarified in ref [81]. As explained above, mixing matrices act as projection operators, and thus have eigenvalues $\lambda \in \{0, 1\}$. Associated with each unit eigenvalue is a combination of kinematic factors of diagrams, accompanied by a superposition of colour factors. These colour factor combinations have the general property that they look like colour factors of *connected* gluon subgraphs. To illustrate this, we may use the two-loop web of figure 14. From eq. (48), we see that the contribution to the exponent from this web is

$$\frac{1}{2} (C(a) - C(b)) (\mathcal{F}(a) - \mathcal{F}(b)), \quad (57)$$

and the fact that there is only one combination of kinematic factors (with accompanying colour factor) is because the web mixing matrix in eq. (49) is of rank 1, i.e. has only one unit eigenvalue. The colour factor appearing in eq. (57) is

$$\mathbf{T}_1^a \mathbf{T}_2^b \mathbf{T}_2^a \mathbf{T}_3^b - \mathbf{T}_1^a \mathbf{T}_2^a \mathbf{T}_2^b \mathbf{T}_3^b = i f^{bacr} \mathbf{T}_1^a \mathbf{T}_2^c \mathbf{T}_3^b, \quad (58)$$

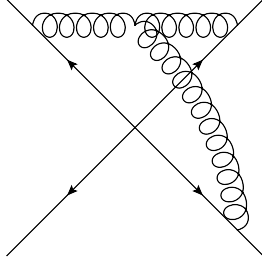


Figure 18: Connected gluon graph connecting three lines at two loops.

where \mathbf{T}_i^a represents a colour generator with adjoint index a on line i , with path ordering outwards from the hard interaction as indicated in figure 14. On the right-hand side we have used the $SU(3)$ colour algebra on line i :

$$\left[\mathbf{T}_i^b, \mathbf{T}_i^c \right] = i f^{bac} \mathbf{T}_i^a, \quad (59)$$

and we see that the surviving colour factor is directly proportional to that of figure 18, which is indeed a connected gluon graph. It should be stressed that it is only the colour factors that are related in this way: in a general gauge, the kinematic combination appearing in eq. (57) is completely different to the kinematic factor of the diagram in figure 18. Nevertheless, this property is a generalisation of a similar property observed for the two-line webs of refs. [66–68], whose colour factors were found to be “maximally non-abelian”, namely equivalent to fully connected graphs.

The fact that only connected colour factors appear in the exponent of the soft function was proven completely generally in ref. [81], for all types of web at arbitrary loop order. To this end, an alternative formalism to the use of web mixing matrices was set up, which involved rewriting replica-ordered Wilson products as single exponential factors, using the Baker-Campbell-Hausdorff formula. Although web mixing matrices do not appear explicitly in this approach, the price one pays is that higher order webs must be calculated with an increasing number of effective vertices describing emission of multiple gluons from each Wilson line. These calculations become cumbersome quickly as the loop order increases. However, the effective vertex formalism provides a well-motivated choice of basis for the connected colour factors appearing at each order [81]. Recently, an alternative approach to calculating soft exponents has appeared, which also involves effective vertices [71, 72]. Interestingly, in this approach the replica trick is not used at all.

The classification of web mixing matrices, and calculation of their associated colour factors, is only part of the story of understanding webs. As eq. (51) makes clear, in order for webs to be useful, one must also calculate the kinematic factors associated with the web Feynman diagrams themselves. This is the subject of the following section.

5 Calculation of webs

As we have seen, web diagrams are Feynman diagrams involving Wilson lines. These can be calculated in either position or momentum space, and the technology needed to perform such calculations has developed over many years (see e.g. [15, 17–19, 55–64, 85–94]). The current state of the art is

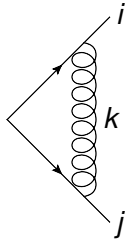


Figure 19: One-loop diagram involving two Wilson lines.

two-loops in full multiparton scattering (for both massless and massive Wilson lines), and three-loops for the case of two Wilson lines.

Wilson line diagrams contain both IR and UV divergences, corresponding to taking gluon subgraphs to infinity, or shrinking them to the origin, respectively. One must then regulate these divergences, and it is conventional to use dimensional regularisation [95] in $4 - 2\epsilon$ dimensions. Here, however, a complication arises: it turns out that, for all Wilson line diagrams at arbitrary loop order, the relevant kinematic integrals vanish. We can see physically why this is by appealing to a one-loop example, namely the diagram of figure 19, which may represent two out of many coloured particles coming from a given hard interaction. Labelling the momentum of line i by p_i , the kinematic part of the diagram is (in momentum space), proportional to

$$\int \frac{d^d k}{(2\pi)^d} \left(\frac{p_i^\mu}{p_i \cdot k} \right) \left(-\frac{\eta_{\mu\nu}}{k^2} \right) \left(-\frac{p_j^\nu}{p_j \cdot k} \right) = \int \frac{d^d k}{(2\pi)^d} \frac{p_i \cdot p_j}{k^2 p_i \cdot k p_j \cdot k}, \quad (60)$$

where we have used the eikonal Feynman rule of eq. (10), and the Feynman gauge gluon propagator. As we saw in section 2, such Feynman rules occur when simplifying the momentum space Feynman rules for whole amplitudes (i.e. with arbitrary k). In particular, we have linearised the denominators associated with the Wilson lines. If they were the usual denominators associated with legs of momentum p_i , eq. (60) would instead read

$$\int \frac{d^d k}{(2\pi)^d} \frac{p_i \cdot p_j}{k^2 [(p_i + k)^2 - m^2] [(p_j - k)^2 - m^2]}, \quad (61)$$

where we have taken the hard particles to be massive for full generality. One may examine the divergence properties of this integral using naïve power counting. This essentially means that we identify k with some momentum scale Λ and see how the integrand behaves as Λ goes to zero (the IR limit) or infinity (the UV limit), ignoring the fact that all quantities are 4-vectors etc. One then finds that eq. (60) goes like Λ^{d-4} and Λ^{d-6} in the IR and UV regimes respectively. This tells us that the integral is logarithmically divergent in Λ in 4 spacetime dimensions in the IR regime, which would show up as a pole in ϵ in dimensional regularisation. On the other hand, there is no UV divergence, due to the terms in the denominators which are quadratic in k^2 .

One finds a different result for the linearised integral of eq. (60), which is logarithmically divergent (in Λ) in both the IR and UV regimes. Comparing the integrals, it is clear why this is: by linearising

the denominators associated with the Wilson lines, one removes the k^2 terms that damp the UV singularity in eq. (61). In other words, by taking the soft limit we have introduced a *spurious* UV singularity. A careful treatment of the integral in eq. (60) shows that these singularities precisely cancel each other, leaving a zero result. Furthermore, this phenomenon generalises to all Wilson line integrals. In other words, the UV singularities of Wilson lines are in one-to-one correspondence with the IR singularities of amplitudes [86]. It follows that we can extract physical information from Wilson line integrals by isolating their UV poles, and ignoring their IR singularities. This can be done using suitable regulators, over and above the use of dimensional regularisation. A particularly convenient regulator has been defined in refs. [55, 56, 82], and consists of replacing the usual QCD Wilson line with

$$\Phi_{\beta_i}^{(m)} = \mathcal{P} \exp \left[ig\mu^\epsilon \int_0^\infty d\lambda \beta_i \cdot A(\lambda\beta_i) e^{-im\lambda\sqrt{\beta_i^2 - i\epsilon}} \right], \quad (62)$$

where we have shown the dependence on the coupling g , which the dimensional regularisation scale μ ensures is dimensionless. Also, β_i is the 4-velocity of the Wilson line, which is assumed to have been tilted off the lightcone if null. Equation (62) differs from the usual Wilson line due to an additional exponential factor, which smoothly cuts off the long-distance contribution to leave only UV poles in ϵ . One recovers the conventional QCD result as $m \rightarrow 0$.

The structure of UV singularities are encoded in a quantity known as the *soft anomalous dimension*. To define this, let us first extract the UV poles of the soft function to define a *renormalised* soft function, that is UV finite:

$$\mathcal{S}_{\text{ren.}} \left(\gamma_{ij}, \alpha_s(\mu^2), \epsilon, \frac{m}{\mu} \right) = \mathcal{S} \left(\gamma_{ij}, \alpha_s(\mu^2), \epsilon, \frac{m}{\mu} \right) Z(\gamma_{ij}, \alpha_s(\mu^2), \epsilon), \quad (63)$$

We have here shown the dependence of each function on the regulators ϵ and m , the coupling α_s and dimensional regularisation scale μ , and the parameters

$$\gamma_{ij} = \frac{2\beta_i \cdot \beta_j}{\sqrt{\beta_i^2} \sqrt{\beta_j^2}} \quad (64)$$

which are related to the hyperbolic angle, in Minkowski space, between any two Wilson lines. In eq. (63), Z is a multiplicative factor that collects all UV counterterms¹¹. Note that this equation is more complicated than it looks: both \mathcal{S} and Z are matrix-valued in the space of colour flows (as discussed in section 4.1), and thus the order of the factors on the right-hand side of eq. (63) is important. The counterterm matrix Z satisfies the renormalisation group equation

$$\mu \frac{d}{d\mu} Z(\gamma_{ij}, \alpha_s(\mu^2), \epsilon) = -Z(\gamma_{ij}, \alpha_s(\mu^2), \epsilon) \Gamma(\gamma_{ij}, \alpha_s(\mu^2)). \quad (65)$$

The factor Γ on the right-hand side is the soft anomalous dimension, and is finite as $\epsilon \rightarrow 0$. Like the counterterm matrix Z , it is matrix-valued in the space of colour flows.

¹¹The fact that Wilson lines renormalise multiplicatively was first shown in refs. [88, 96–98].

For practical calculational purposes, there is a direct route from the unrenormalised soft function (in terms of webs) to the soft anomalous dimension. One may write the former as

$$\mathcal{S}(\alpha_s, \epsilon) = \exp \left[\sum_{n=1}^{\infty} \sum_{k=-n}^{\infty} \alpha_s^n \epsilon^k w^{(n,k)} \right], \quad (66)$$

where $w^{(n,k)}$ is the coefficient of ϵ^k from the sum of all web contributions at $\mathcal{O}(\alpha_s^n)$. In terms of these coefficients, the soft anomalous dimension is given up to three-loop order by [82]

$$\begin{aligned} \Gamma^{(1)} &= -2w^{(1,-1)}, \\ \Gamma^{(2)} &= -4w^{(2,-1)} - 2 \left[w^{(1,-1)}, w^{(1,0)} \right], \\ \Gamma^{(3)} &= -6w^{(3,-1)} + \frac{3}{2}b_0 \left[w^{(1,-1)}, w^{(1,1)} \right] + 3 \left[w^{(1,0)}, w^{(2,-1)} \right] + 3 \left[w^{(2,0)}, w^{(1,-1)} \right] \\ &\quad + \left[w^{(1,0)}, \left[w^{(1,-1)}, w^{(1,0)} \right] \right] - \left[w^{(1,-1)}, \left[w^{(1,-1)}, w^{(1,1)} \right] \right], \end{aligned} \quad (67)$$

where $\Gamma^{(i)}$ is the coefficient of α_s^i in the soft anomalous dimension, and b_0 the one-loop coefficient of the QCD β function. We see a very general structure, namely that the coefficients of Γ consist of the single pole of the unrenormalised webs at each given order, dressed by commutators of lower-order web coefficients. These commutators are non-zero precisely because webs are matrix-valued in the space of colour flows. When this complication is absent (such as in two line scattering, or multiparton scattering in the limit of a large number of colours), these commutators disappear. This is intimately related to the fact that webs in two-parton scattering (in the language of refs. [66–68]) are single irreducible diagrams. Such diagrams have a single divergence at arbitrary loop order, such that the soft anomalous dimension (also known as the cusp anomalous dimension in this case) inherits all of its information from the coefficient of the single pole in each web. For multiparton webs, diagrams can instead be reducible, meaning that they have higher order poles in ϵ . These are then cancelled by commutators of lower order webs, in a tightly constrained way.

Problem 7. Consider the two-loop web of figure 14. Identify the single connected colour factor that this contributes to. Identify also the lower order webs that enter the subtraction term for this web, and show that they give rise to the same colour factor.

The combination of an unrenormalised web with its commutator contributions has been called a *subtracted web* in refs. [55, 56, 82], and has a number of special properties. Firstly, dependence on the regulator m used to separate IR and UV singularities cancels only at the level of subtracted webs. Secondly, the analytic functions of cusp angles that appear in subtracted webs are much simpler than for unsubtracted webs. A crucial property in making the web language useful is that subtraction terms operate on a web-by-web basis. That is, each closed set of web diagrams interacts with subtraction terms involving lower order diagrams from the *same* set, such that webs do not mix with each other under renormalisation. It is for this reason that the identification of webs as closed sets of diagrams is meaningful. Different webs would still mix with each other, however, under gauge transformations. Clever gauge choices can perhaps be used to simplify the calculation of webs at higher orders e.g. the conformal gauges of ref. [99].

Based on the above discussion, the procedure for calculating the soft anomalous dimension matrix at a given order is as follows:

1. Choose a basis of independent connected colour factors.
2. For each web, find (using the web mixing matrix or otherwise) the combination of kinematic factors accompanying each connected colour factor, if present. Note that the fact that only combinations are needed as opposed to individual diagrams potentially leads to simplifications, due to cancellations between diagrams at the integrand level.
3. Calculate each kinematic combination, including all relevant commutator subtraction terms. Further simplifications occur at this point, including independence of the regulator used to separate UV and IR singularities.
4. Finally, add together all kinematic combinations for a given connected colour factor. This gives a gauge-invariant contribution to the soft anomalous dimension.

This programme of work is currently being carried out at three-loop order, where webs may be classified according to the number of three and four gluon vertices off the Wilson lines. Diagrams with no multigluon vertices are known as *Multiple Gluon Exchange Webs* (MGEWs). Explicit results have been presented for all three-loop examples connecting three or more lines [55, 56], and the two-line case has been studied in ref. [61]. Certain diagrams of this type can even be calculated to all orders i.e. for any number of gluons [56]. This mirrors parallel developments (discussed above) in the combinatoric understanding of web mixing matrices, and suggests that it may be possible to understand all-order properties in the exponent of the soft amplitude. As an example, ref. [56] conjectures a basis of functions which are believed to be adequate to describe the result of any MGEW, at arbitrary loop order. This basis, or generalisations thereof, may also hold for more complicated web types. An important element in the construction of this basis is the efficient characterisation of analytic properties using the *Symbol* of refs. [100–103], which tool will doubtless prove to be useful at higher loop orders. Very recently, the calculation of the fully connected webs linking four Wilson lines has been completed [104], in the lightlike limit. As argued by the authors, this is sufficient to obtain the complete soft anomalous dimension in this limit at three-loop order. Another interesting recent development is the use of unitarity-inspired methods to compute webs [57, 58].

6 Conclusion

In this article, we have provided a review of past and current developments in the classification of infrared singularities in scattering amplitudes. These are interesting for a variety of phenomenological and formal reasons, and we have focused mainly on the case of non-abelian gauge theories, whose singularity structure is much richer than QED or gravity.

Our main aim has been to provide an accessible introduction to the language of *webs*, namely Feynman diagrams that occur in the exponent of the soft (infrared divergent) part of an amplitude, itself a vacuum expectation value of Wilson lines. We have seen that webs in multiparton scattering are closed sets of diagrams, related by permutations of gluons on the Wilson lines. The colour and kinematic parts of these diagrams are entangled by *web mixing matrices*, whose mathematical

structure makes contact with interesting problems in contemporary combinatorial research. Further elucidation of these matrices, from either a physics or mathematics viewpoint, offers significant insights into the all-order properties of perturbation theory. This is equally true for the calculation of the kinematic parts of web diagrams, where systematic methods are beginning to be developed.

Investigation of multiparton webs, and their associated physics in a variety of gauge theories, is still a very young subject. Many interesting results are still ripe to be discovered, and work towards such discoveries is ongoing!

Acknowledgments

I am grateful to Stefano Forte for the suggestion and invitation to publish these notes. My knowledge of this subject has benefited greatly over the last few years from conversations and collaborations with Mark Dukes, Giulio Falcioni, Einan Gardi, Mark Harley, Eric Laenen, Lorenzo Magnea, Heather McAslan, Darren Scott, Jenni Smillie, Gerben Stavenga and Einar Steingrímsson. I am supported by the UK Science and Technology Facilities Council (STFC), under grant ST/L000446/1.

References

- [1] F. Bloch and A. Nordsieck, “Note on the Radiation Field of the electron,” *Phys.Rev.* **52** (1937) 54–59.
- [2] G. F. Sterman, “Summation of Large Corrections to Short Distance Hadronic Cross-Sections,” *Nucl. Phys.* **B281** (1987) 310.
- [3] S. Catani and L. Trentadue, “Resummation of the QCD Perturbative Series for Hard Processes,” *Nucl. Phys.* **B327** (1989) 323.
- [4] H. Contopanagos, E. Laenen, and G. Sterman, “Sudakov factorization and resummation,” *Nucl. Phys.* **B484** (1997) 303–330, [hep-ph/9604313](#).
- [5] G. P. Korchemsky and G. Marchesini, “Resummation of large infrared corrections using Wilson loops,” *Phys. Lett.* **B313** (1993) 433–440.
- [6] G. P. Korchemsky and G. Marchesini, “Structure function for large x and renormalization of wilson loop,” *Nucl. Phys.* **B406** (1993) 225–258, [hep-ph/9210281](#).
- [7] S. Forte and G. Ridolfi, “Renormalization group approach to soft gluon resummation,” *Nucl. Phys.* **B650** (2003) 229–270, [hep-ph/0209154](#).
- [8] T. Becher and M. Neubert, “Threshold resummation in momentum space from effective field theory,” *Phys. Rev. Lett.* **97** (2006) 082001, [hep-ph/0605050](#).
- [9] M. D. Schwartz, “Resummation and NLO matching of event shapes with effective field theory,” *Phys.Rev.* **D77** (2008) 014026, [0709.2709](#).
- [10] C. W. Bauer, S. P. Fleming, C. Lee, and G. F. Sterman, “Factorization of $e+e-$ Event Shape Distributions with Hadronic Final States in Soft Collinear Effective Theory,” *Phys.Rev.* **D78** (2008) 034027, [0801.4569](#).

- [11] J.-y. Chiu, A. Fuhrer, R. Kelley, and A. V. Manohar, “Factorization Structure of Gauge Theory Amplitudes and Application to Hard Scattering Processes at the LHC,” *Phys.Rev.* **D80** (2009) 094013, 0909.0012.
- [12] E. Laenen, G. Stavenga, and C. D. White, “Path integral approach to eikonal and next-to-eikonal exponentiation,” *JHEP* **03** (2009) 054, 0811.2067.
- [13] T. Becher, A. Broggio, and A. Ferroglia, “Introduction to Soft-Collinear Effective Theory,” 1410.1892.
- [14] G. Luisoni and S. Marzani, “Resummation in QCD,” 1505.04084.
- [15] E. Gardi and L. Magnea, “Factorization constraints for soft anomalous dimensions in QCD scattering amplitudes,” *JHEP* **0903** (2009) 079, 0901.1091.
- [16] E. Gardi and L. Magnea, “Infrared singularities in QCD amplitudes,” *Nuovo Cim.* **032C** (2009) 137–157, 0908.3273.
- [17] T. Becher and M. Neubert, “Infrared singularities of scattering amplitudes in perturbative QCD,” *Phys. Rev. Lett.* **102** (2009) 162001, 0901.0722.
- [18] T. Becher and M. Neubert, “On the Structure of Infrared Singularities of Gauge-Theory Amplitudes,” *JHEP* **06** (2009) 081, 0903.1126.
- [19] T. Becher and M. Neubert, “Infrared singularities of QCD amplitudes with massive partons,” *Phys. Rev.* **D79** (2009) 125004, 0904.1021.
- [20] Z. Bern, T. Dennen, Y.-t. Huang, and M. Kiermaier, “Gravity as the Square of Gauge Theory,” *Phys.Rev.* **D82** (2010) 065003, 1004.0693.
- [21] Z. Bern, J. J. M. Carrasco, and H. Johansson, “Perturbative Quantum Gravity as a Double Copy of Gauge Theory,” *Phys.Rev.Lett.* **105** (2010) 061602, 1004.0476.
- [22] Z. Bern, “Perturbative quantum gravity and its relation to gauge theory,” *Living Rev.Rel.* **5** (2002) 5, gr-qc/0206071.
- [23] C. Boucher-Veronneau and L. Dixon, “ $N = 4$ Supergravity Amplitudes from Gauge Theory at Two Loops,” 1110.1132. * Temporary entry *.
- [24] S. G. Naculich, H. Nastase, and H. J. Schnitzer, “Linear relations between $N = 4$ supergravity and subleading-color SYM amplitudes,” 1111.1675. * Temporary entry *.
- [25] S. G. Naculich, H. Nastase, and H. J. Schnitzer, “Applications of Subleading Color Amplitudes in $N=4$ SYM Theory,” 1105.3718.
- [26] S. Weinberg, “Infrared photons and gravitons,” *Phys.Rev.* **140** (1965) B516–B524.
- [27] S. G. Naculich and H. J. Schnitzer, “Eikonal methods applied to gravitational scattering amplitudes,” *JHEP* **1105** (2011) 087, 1101.1524. * Temporary entry *.
- [28] C. D. White, “Factorization Properties of Soft Graviton Amplitudes,” *JHEP* **1105** (2011) 060, 1103.2981.

- [29] R. Akhoury, R. Saotome, and G. Sterman, “Collinear and Soft Divergences in Perturbative Quantum Gravity,” 1109.0270.
- [30] M. Beneke and G. Kirilin, “Soft-collinear gravity,” *JHEP* **1209** (2012) 066, 1207.4926.
- [31] S. Oxburgh and C. White, “BCJ duality and the double copy in the soft limit,” *JHEP* **1302** (2013) 127, 1210.1110.
- [32] A. H. Mueller, “On the asymptotic behavior of the Sudakov form-factor,” *Phys.Rev.* **D20** (1979) 2037.
- [33] J. C. Collins, “Algorithm to compute corrections to the Sudakov form-factor,” *Phys.Rev.* **D22** (1980) 1478.
- [34] A. Sen, “Asymptotic Behavior of the Sudakov Form-Factor in QCD,” *Phys.Rev.* **D24** (1981) 3281.
- [35] G. Korchemsky, “Double logarithmic asymptotics in QCD,” *Phys.Lett.* **B217** (1989) 330–334.
- [36] J. C. Collins, “Sudakov form-factors,” *Adv.Ser.Direct.High Energy Phys.* **5** (1989) 573–614, hep-ph/0312336.
- [37] L. Magnea and G. F. Sterman, “Analytic continuation of the Sudakov form-factor in QCD,” *Phys.Rev.* **D42** (1990) 4222–4227.
- [38] L. J. Dixon, L. Magnea, and G. Sterman, “Universal structure of subleading infrared poles in gauge theory amplitudes,” *JHEP* **08** (2008) 022, 0805.3515.
- [39] Y. L. Dokshitzer, G. Marchesini, and G. P. Salam, “Revisiting parton evolution and the large-x limit,” *Phys. Lett.* **B634** (2006) 504–507, hep-ph/0511302.
- [40] E. Laenen, L. Magnea, and G. Stavenga, “On next-to-eikonal corrections to threshold resummation for the Drell-Yan and DIS cross sections,” *Phys. Lett.* **B669** (2008) 173–179, 0807.4412.
- [41] S. Moch and A. Vogt, “Threshold Resummation of the Structure Function $F(L)$,” *JHEP* **0904** (2009) 081, 0902.2342.
- [42] G. Grunberg and V. Ravindran, “On threshold resummation beyond leading 1-x order,” *JHEP* **0910** (2009) 055, 0902.2702.
- [43] S. Moch and A. Vogt, “On non-singlet physical evolution kernels and large-x coefficient functions in perturbative QCD,” *JHEP* **0911** (2009) 099, 0909.2124.
- [44] G. Soar, S. Moch, J. Vermaseren, and A. Vogt, “On Higgs-exchange DIS, physical evolution kernels and fourth-order splitting functions at large x,” *Nucl.Phys.* **B832** (2010) 152–227, 0912.0369.
- [45] E. Laenen, L. Magnea, G. Stavenga, and C. D. White, “Next-to-eikonal corrections to soft gluon radiation: a diagrammatic approach,” *JHEP* **1101** (2011) 141, 1010.1860.

- [46] A. Almasy, G. Soar, and A. Vogt, “Generalized double-logarithmic large-x resummation in inclusive deep-inelastic scattering,” *JHEP* **1103** (2011) 030, 1012.3352.
- [47] R. D. Ball, M. Bonvini, S. Forte, S. Marzani, and G. Ridolfi, “Higgs production in gluon fusion beyond NNLO,” *Nucl.Phys.* **B874** (2013) 746–772, 1303.3590.
- [48] T. Altinoluk, N. Armesto, G. Beuf, M. Martínez, and C. A. Salgado, “Next-to-eikonal corrections in the CGC: gluon production and spin asymmetries in pA collisions,” *JHEP* **1407** (2014) 068, 1404.2219.
- [49] L. Apolinario, N. Armesto, J. G. Milhano, and C. A. Salgado, “Medium-induced gluon radiation and colour decoherence beyond the soft approximation,” 1407.0599.
- [50] D. de Florian, J. Mazzitelli, S. Moch, and A. Vogt, “Approximate N³LO Higgs-boson production cross section using physical-kernel constraints,” 1408.6277.
- [51] N. Lo Presti, A. Almasy, and A. Vogt, “Leading large-x logarithms of the quark & gluon contributions to inclusive Higgs-boson and lepton-pair production,” *Phys.Lett.* **B737** (2014) 120–123, 1407.1553.
- [52] D. Bonocore, E. Laenen, L. Magnea, L. Vernazza, and C. D. White, “The method of regions and next-to-soft corrections in DrellYan production,” *Phys.Lett.* **B742** (2015) 375–382, 1410.6406.
- [53] D. Bonocore, E. Laenen, L. Magnea, S. Melville, L. Vernazza, *et al.*, “A factorization approach to next-to-leading-power threshold logarithms,” *JHEP* **1506** (2015) 008, 1503.05156.
- [54] C. White, “Diagrammatic insights into next-to-soft corrections,” *Phys.Lett.* **B737** (2014) 216–222, 1406.7184.
- [55] E. Gardi, “From Webs to Polylogarithms,” *JHEP* **1404** (2014) 044, 1310.5268.
- [56] G. Falcioni, E. Gardi, M. Harley, L. Magnea, and C. D. White, “Multiple Gluon Exchange Webs,” *JHEP* **1410** (2014) 10, 1407.3477.
- [57] E. Laenen, K. J. Larsen, and R. Rietkerk, “Position-space cuts for Wilson line correlators,” 1505.02555.
- [58] E. Laenen, K. J. Larsen, and R. Rietkerk, “Imaginary parts and discontinuities of Wilson line correlators,” *Phys.Rev.Lett.* **114** (2015), no. 18, 181602, 1410.5681.
- [59] A. Grozin, J. M. Henn, G. P. Korchemsky, and P. Marquard, “Three Loop Cusp Anomalous Dimension in QCD,” *Phys.Rev.Lett.* **114** (2015), no. 6, 062006, 1409.0023.
- [60] A. Grozin, J. M. Henn, G. P. Korchemsky, and P. Marquard, “The n_f terms of the three-loop cusp anomalous dimension in QCD,” *PoS LL2014* (2014) 016, 1406.7828.
- [61] J. M. Henn and T. Huber, “The four-loop cusp anomalous dimension in $\mathcal{N} = 4$ super Yang-Mills and analytic integration techniques for Wilson line integrals,” *JHEP* **1309** (2013) 147, 1304.6418.

- [62] J. M. Henn and T. Huber, “Systematics of the cusp anomalous dimension,” *JHEP* **1211** (2012) 058, 1207.2161.
- [63] D. Correa, J. Henn, J. Maldacena, and A. Sever, “The cusp anomalous dimension at three loops and beyond,” *JHEP* **1205** (2012) 098, 1203.1019.
- [64] D. Correa, J. Henn, J. Maldacena, and A. Sever, “An exact formula for the radiation of a moving quark in N=4 super Yang Mills,” *JHEP* **1206** (2012) 048, 1202.4455.
- [65] D. R. Yennie, S. C. Frautschi, and H. Suura, “The infrared divergence phenomena and high-energy processes,” *Ann. Phys.* **13** (1961) 379–452.
- [66] J. Gatheral, “Exponentiation of eikonal cross-sections in nonabelian gauge theories,” *Phys.Lett.* **B133** (1983) 90.
- [67] J. Frenkel and J. Taylor, “Nonabelian eikonal exponentiation,” *Nucl.Phys.* **B246** (1984) 231.
- [68] G. F. Sterman, “Infrared divergences in perturbative QCD. (talk),” *AIP Conf.Proc.* **74** (1981) 22–40.
- [69] C. F. Berger, “Soft gluon exponentiation and resummation,” hep-ph/0305076. Ph.D. Thesis (Advisor: George Sterman).
- [70] A. Mitov, G. Sterman, and I. Sung, “Diagrammatic Exponentiation for Products of Wilson Lines,” *Phys.Rev.* **D82** (2010) 096010, 1008.0099.
- [71] A. Vladimirov, “Generating function for web diagrams,” *Phys.Rev.* **D90** (2014), no. 6, 066007, 1406.6253.
- [72] A. A. Vladimirov, “Exponentiation for products of Wilson lines within the generating function approach,” 1501.03316.
- [73] D. Miller and C. White, “The Gravitational cusp anomalous dimension from AdS space,” *Phys.Rev.* **D85** (2012) 104034, 1201.2358.
- [74] S. Melville, S. Naculich, H. Schnitzer, and C. White, “Wilson line approach to gravity in the high energy limit,” *Phys.Rev.* **D89** (2014) 025009, 1306.6019.
- [75] G. P. Korchemsky and G. Marchesini, “Structure function for large x and renormalization of Wilson loop,” *Nucl. Phys.* **B406** (1993) 225–258, hep-ph/9210281.
- [76] M. Mezard, G. Parisi, and M. Virasoro, “Spin Glass Theory and Beyond,” World Scientific (1987) 476pp.
- [77] E. Gardi, E. Laenen, G. Stavenga, and C. D. White, “Webs in multiparton scattering using the replica trick,” *JHEP* **1011** (2010) 155, 1008.0098.
- [78] M. Sjö Dahl, “Color evolution of $2 \rightarrow 3$ processes,” *JHEP* **0812** (2008) 083, 0807.0555.
- [79] M. Sjö Dahl, “Color structure for soft gluon resummation: A General recipe,” *JHEP* **0909** (2009) 087, 0906.1121.

- [80] E. Gardi and C. D. White, “General properties of multiparton webs: Proofs from combinatorics,” *JHEP* **1103** (2011) 079, 1102.0756.
- [81] E. Gardi, J. M. Smillie, and C. D. White, “The Non-Abelian Exponentiation theorem for multiple Wilson lines,” *JHEP* **1306** (2013) 088, 1304.7040.
- [82] E. Gardi, J. M. Smillie, and C. D. White, “On the renormalization of multiparton webs,” *JHEP* **1109** (2011) 114, 1108.1357.
- [83] M. Dukes, E. Gardi, E. Steingrimsson, and C. D. White, “Web worlds, web-colouring matrices, and web-mixing matrices,” *J.Comb.Theory Ser.* **A120** (2013) 1012–1037, 1301.6576.
- [84] M. Dukes, E. Gardi, H. McAslan, D. J. Scott, and C. D. White, “Webs and Posets,” *JHEP* **1401** (2014) 024, 1310.3127.
- [85] G. Korchemsky and A. Radyushkin, “Loop Space Formalism and Renormalization Group for the Infrared Asymptotics of QCD,” *Phys.Lett.* **B171** (1986) 459–467.
- [86] G. Korchemsky and A. Radyushkin, “Renormalization of the Wilson Loops Beyond the Leading Order,” *Nucl.Phys.* **B283** (1987) 342–364.
- [87] G. Korchemsky and A. Radyushkin, “Infrared asymptotics of perturbative QCD: Renormalization properties of the Wilson loops in higher orders of perturbation theory,” *Sov.J.Nucl.Phys.* **44** (1986) 877.
- [88] R. A. Brandt, F. Neri, and M.-a. Sato, “Renormalization of Loop Functions for All Loops,” *Phys.Rev.* **D24** (1981) 879.
- [89] S. M. Aybat, L. J. Dixon, and G. F. Sterman, “The Two-loop anomalous dimension matrix for soft gluon exchange,” *Phys.Rev.Lett.* **97** (2006) 072001, hep-ph/0606254.
- [90] S. M. Aybat, L. J. Dixon, and G. F. Sterman, “The Two-loop soft anomalous dimension matrix and resummation at next-to-next-to leading pole,” *Phys.Rev.* **D74** (2006) 074004, hep-ph/0607309.
- [91] N. Kidonakis, “Two-loop soft anomalous dimensions and NNLL resummation for heavy quark production,” *Phys.Rev.Lett.* **102** (2009) 232003, 0903.2561.
- [92] A. Ferroglia, M. Neubert, B. D. Pecjak, and L. L. Yang, “Two-loop divergences of massive scattering amplitudes in non-abelian gauge theories,” *JHEP* **0911** (2009) 062, 0908.3676.
- [93] A. Ferroglia, M. Neubert, B. D. Pecjak, and L. L. Yang, “Two-loop divergences of scattering amplitudes with massive partons,” *Phys.Rev.Lett.* **103** (2009) 201601, 0907.4791.
- [94] A. Mitov, G. F. Sterman, and I. Sung, “The Massive Soft Anomalous Dimension Matrix at Two Loops,” *Phys.Rev.* **D79** (2009) 094015, 0903.3241.
- [95] G. ’t Hooft and M. Veltman, “Regularization and Renormalization of Gauge Fields,” *Nucl.Phys.* **B44** (1972) 189–213.

- [96] A. M. Polyakov, “Gauge Fields as Rings of Glue,” *Nucl.Phys.* **B164** (1980) 171–188.
- [97] I. Y. Arefeva, “Quantum contour field equations,” *Phys.Lett.* **B93** (1980) 347–353.
- [98] V. Dotsenko and S. Vergeles, “Renormalizability of Phase Factors in the Nonabelian Gauge Theory,” *Nucl.Phys.* **B169** (1980) 527.
- [99] Y.-T. Chien, M. D. Schwartz, D. Simmons-Duffin, and I. W. Stewart, “Jet Physics from Static Charges in AdS,” *Phys.Rev.* **D85** (2012) 045010, 1109.6010.
- [100] A. Goncharov, “A simple construction of Grassmannian polylogarithms,” 0908.2238.
- [101] A. B. Goncharov, M. Spradlin, C. Vergu, and A. Volovich, “Classical Polylogarithms for Amplitudes and Wilson Loops,” *Phys.Rev.Lett.* **105** (2010) 151605, 1006.5703.
- [102] C. Duhr, H. Gangl, and J. R. Rhodes, “From polygons and symbols to polylogarithmic functions,” *JHEP* **1210** (2012) 075, 1110.0458.
- [103] C. Duhr, “Hopf algebras, coproducts and symbols: an application to Higgs boson amplitudes,” *JHEP* **1208** (2012) 043, 1203.0454.
- [104] Ø. Almelid, C. Duhr, and E. Gardi, “Three-loop corrections to the soft anomalous dimension in multi-leg scattering,” 1507.00047.